

# Practical guides for x-ray photoelectron spectroscopy (XPS): Interpreting the carbon 1s spectrum

Cite as: J. Vac. Sci. Technol. A **39**, 013204 (2021); <https://doi.org/10.1116/6.0000682>

Submitted: 30 September 2020 . Accepted: 07 December 2020 . Published Online: 06 January 2021

 Thomas R. Gengenbach,  George H. Major,  Matthew R. Linford, and  Christopher D. Easton

## COLLECTIONS

Paper published as part of the special topic on [Special Topic Collection: Reproducibility Challenges and Solutions](#)



View Online



Export Citation



CrossMark

## ARTICLES YOU MAY BE INTERESTED IN

[Practical guide for curve fitting in x-ray photoelectron spectroscopy](#)

Journal of Vacuum Science & Technology A **38**, 061203 (2020); <https://doi.org/10.1116/6.0000377>

[Practical guides for x-ray photoelectron spectroscopy: Quantitative XPS](#)

Journal of Vacuum Science & Technology A **38**, 041201 (2020); <https://doi.org/10.1116/1.5141395>

[Practical guide to the use of backgrounds in quantitative XPS](#)

Journal of Vacuum Science & Technology A **39**, 011201 (2021); <https://doi.org/10.1116/6.0000661>



Advance your science and  
career as a member of

**AVS**

LEARN MORE



# Practical guides for x-ray photoelectron spectroscopy (XPS): Interpreting the carbon 1s spectrum

Cite as: J. Vac. Sci. Technol. A 39, 013204 (2021); doi: 10.1116/6.0000682

Submitted: 30 September 2020 · Accepted: 7 December 2020 ·

Published Online: 6 January 2021



Thomas R. Gengenbach,<sup>1,a)</sup> George H. Major,<sup>2</sup> Matthew R. Linford,<sup>2,a)</sup> and Christopher D. Easton<sup>1,a)</sup>

## AFFILIATIONS

<sup>1</sup>Commonwealth Scientific and Industrial Research Organisation (CSIRO) Manufacturing, Clayton, Victoria 3168, Australia

<sup>2</sup>Department of Chemistry and Biochemistry, Brigham Young University, Provo, Utah 84602

**Note:** This paper is part of the Special Topic Collection on Reproducibility Challenges and Solutions.

**Electronic addresses:** [thomas.gengenbach@csiro.au](mailto:thomas.gengenbach@csiro.au), [chris.easton@csiro.au](mailto:chris.easton@csiro.au), [mrlinford@chem.byu.edu](mailto:mrlinford@chem.byu.edu)

## ABSTRACT

The carbon 1s photoelectron spectrum is the most widely fit and analyzed narrow scan in the x-ray photoelectron spectroscopy (XPS) literature. It is, therefore, critically important to adopt well-established protocols based on best practices for its analysis, since results of these efforts affect research outcomes in a wide range of different application areas across materials science. Unfortunately, much XPS peak fitting in the scientific literature is inaccurate. In this guide, we describe and explain the most common problems associated with C 1s narrow scan analysis in the XPS literature. We then provide an overview of rules, principles, and considerations that, taken together, should guide the approach to the analysis of C 1s spectra. We propose that following this approach should result in (1) the avoidance of common problems and (2) the extraction of reliable, reproducible, and meaningful information from experimental data.

Published under license by AVS. <https://doi.org/10.1116/6.0000682>

## I. INTRODUCTION

Carbon is not particularly abundant in the Earth's crust. With an estimated concentration of several hundred to thousand parts per million (ppm) by weight, it does not even rank among the top ten most abundant elements. However, it is ubiquitous at the Earth's surface, i.e., the human environment, in solid, liquid, or gaseous form. In spite of carbon's relatively low overall abundance, its importance cannot be overstated. Unlike most elements, carbon readily bonds to itself to form stable single, double, and triple bonds, forming chains and rings, and combining with other elements in a way that produces an essentially infinite number of organic compounds with molecular weights that range from little more than a dozen to millions of atomic mass units (amu or g/mol). Accordingly, it is rare in the day-to-day work of an analytical laboratory to study samples that do not contain carbon in some form. This is particularly true for surface analytical laboratories that use highly surface-sensitive techniques such as x-ray photoelectron spectroscopy (XPS) to characterize materials. This carbon at sample surfaces (or in the bulk in an XPS depth profile) has many potential sources:

- The material itself may be carbonaceous. Such materials include graphitic carbon, e.g., graphene and carbon nanotubes; organic materials, such as many polymers and self-assembled monolayers; and diamond (and doped diamond).
- The material may be a hybrid of inorganic and organic constituents, either by nature or by design, e.g., metal organic frameworks and carbon steel.
- Organic impurities, either in the bulk or as surface contamination, the latter typically known as adventitious carbon (AdC).

The presence of carbon in XPS analyses is both directly and indirectly felt. Carbon may perturb (chemically shift) the peak positions of other elements to which it is bonded. The valence band signals from carbon-containing surfaces/materials, i.e., the signals at binding energies (BE) of ~0–30 eV, are a direct result of carbon in chemical bonds and often constitute a “fingerprint” for a material. Even if only to a small degree, AdC attenuates the XPS signals that originate below it. Carbon also produces a strong Auger signal, which is fairly broad but often ignored because of its complexity. Nevertheless, in spite of the usefulness, or potential

usefulness, of these other signals, it is the C 1s peak envelope in XPS that is almost always the most important signal for understanding carbon at surfaces and materials. Some unique and useful features/advantages of the C 1s envelope are as follows. The C 1s core electrons have a large cross section (they produce a strong signal) when excited by the Al K $\alpha$  and Mg K $\alpha$  x-ray lines that are used in most lab-based XPS instruments. Appearing at  $\sim 285$  eV, the C 1s envelope does not overlap with most other XPS signals. Carbon in the C 1s envelope is chemically shifted over quite a wide range ( $\sim 10$  eV) by the elements it binds to, which allows effective peak fitting and oxidation state identification. The C 1s signals of many materials are well understood, and this understanding is very often applied successfully to new materials. C 1s peak fitting, if appropriately done, can yield good results without advanced calculations (only modestly priced peak fitting software is required). Finally, as a first approximation, the C 1s signal from AdC is a convenient signal for correcting the binding energy (BE) scale in an XPS spectrum to account for sample charging. Of course, this approach may not give exact binding energies for signals.<sup>1</sup> Nevertheless, for many materials, it facilitates accurate peak identification, which is all that is needed in many cases. Therefore, it is not surprising that both the qualitative and quantitative analyses of C 1s narrow scans features very prominently in XPS research; the C 1s narrow scan is generally the most information-rich and instructive spectrum in an analysis of a carbon-containing material, and often the only one needed to obtain the desired information. In addition, even if the focus of a scientific investigation is exclusively on inorganic materials, the presence of carbon will usually have to be accounted for when processing and interpreting the data. For example, when studying metal oxides, one must consider the inevitable presence of organic contaminants, which almost always have carbon-oxygen functional groups. This contamination will affect interpretation of the elemental composition of the material and the O 1s signal.

For years, the worldwide community of XPS experts has been expressing increasing concern about inaccurate XPS peak fitting and analysis that have been entering the scientific literature. To better quantify and understand this problem, the authors of this work recently published an evaluation of the XPS spectra published over a 6-month period in three high-quality journals.<sup>2</sup> Part of this study included an investigation of the elements that are most frequently researched for XPS at an online database and shown in the literature as narrow scans. This analysis revealed that carbon and then oxygen are the top two elements on both lists. Unfortunately, this study also revealed a high frequency of problems and errors associated with the analysis of the C 1s signal. In many cases, these errors seriously undermined and often completely invalidated the reported conclusions of the papers.<sup>2</sup> The increasing frequency of flawed and incorrect analysis is not restricted to the analysis of XPS, including the C 1s narrow scan, but is just one facet of a much wider and very serious problem in the scientific literature, usually referred to as the reproducibility crisis.<sup>3–5</sup>

To address these serious problems, in science generally and in XPS research specifically, a collaboration of international subject-matter experts and journal editors have begun to raise public awareness and develop and publish a series of relevant guides and tutorials.<sup>6,7</sup> Several of the latter have already been published in a

Special Topic Collection (“Reproducibility Challenges and Solutions”) of the *Journal of Vacuum Science and Technology A*.<sup>8</sup> The objective of this present guide is to provide practical guidance in acquiring, processing, and interpreting carbon 1s spectra and associated data based on current best practices. This work is not intended to be a comprehensive and detailed instruction manual but rather a summary of the principles underlying the analysis of C 1s spectra and of the problems and pitfalls one might encounter while studying them. Throughout this guide, we will refer to previous publications that provide examples and highlight specific, useful aspects of the C 1s analysis. The reader that is less familiar with XPS is referred to Stevie and Donley’s introductory guide to the technique.<sup>9</sup>

The target audience of this paper is researchers with at least a minimal level of expertise and practical experience with XPS, although we would anticipate that researchers at all levels of experience will find this information to be useful.

This guide is divided into two sections. In the first, we list the most common problems associated with the analysis of C 1s spectra in the literature. In the second, we provide an overview of rules, principles, and considerations that, taken together, should guide an approach to the analysis of C 1s spectra. We propose that following these guidelines should result in (1) avoiding common problems and (2) the extraction of reliable and meaningful information from experimental data. In the appendices, we present examples and case studies to illustrate some of the common problems that are identified in the first section (Appendices A–C) and a compilation of reference values for C 1s chemical shifts (Appendix D).

## II. STATING THE PROBLEM

While C 1s spectra are investigated in many very different areas of research, most errors and problems found in the published XPS literature can be grouped into one or more of the following categories.

### A. Lack of appropriate error analysis

A lack of appropriate error analysis is one of the most common problems found in scientific publications. It lies at the heart of all other problems listed below. Every experimental technique and every data processing method is associated with a range of uncertainties that must be considered when interpreting the results. Careful analysis is required of every step of an experimental protocol to estimate the uncertainty introduced during that step, and, finally, the total error associated with obtaining a particular result. An example of the poor error analysis in XPS is for authors to report too many significant figures in their results. For example, synthetic (mathematically derived) peak areas, widths, and positions are sometimes reported with five or six significant figures. In some cases, these results come from single analyses of a sample, where, to make things worse, these analyses may be of broad peak envelopes fit with multiple synthetic components, i.e., there is often significant uncertainty in these analyses. The complete statement of a measured value should include an estimate of the level of confidence associated with that value. Properly reporting an experimental result, along with its uncertainty, allows the reader to assess the quality of the experiment and permits meaningful comparisons

with other similar values or a theoretical prediction. Without reporting experimental uncertainties or errors, a measurement becomes meaningless because it cannot reliably be interpreted. This is particularly important in analyzing XPS data, specifically C 1s spectra: typical chemical shifts of C 1s signals are of the order of a few eV and often only 1 eV or less. When those values are compared with the typical, measured peak widths of 0.5–2.0 eV from pure samples/components, it becomes clear why curve-fitting is one of the most important and wide-spread data processing methods used in the C 1s analysis: it is really the only method that enables the analyst to identify and quantify several overlapping spectral peaks. However, depending on the specific protocol used, curve-fitting is associated with significant uncertainties that affect the accuracy/precision and reliability of the result. While an analysis will ideally include data from replicate samples with the use of appropriate statistics to summarize the results, at the very least, authors should be able to analyze multiple spots on most surfaces and provide averages and standard deviations for these results.

## B. Overfitting

Overfitting refers to a tendency to use more fit components for a curve-fit than can be reasonably justified based on the quality of the raw data (resolution, signal/noise ratio) and the sample chemistry. For example, in analyzing complex polymeric systems that are expected to have a range of different functional groups, one may be tempted to include separate fit components for each of the expected functionalities and to constrain their respective peak energies to reference values taken from a database. One commonly sees examples of this approach in the literature, even in cases when there is no specific spectral feature of C 1s that might define any particular component peak. This approach may be justified if only carbon-carbon and carbon-oxygen functional groups are present since these fall into five reasonably clear categories: (1) C–C/C–H based, (2) C–O based, (3) C=O or O–C–O based, (4) O–C=O based, and (5) O–C(O)–O based. The respective C 1s peaks of these components are well separated in energy by about 1.2–1.5 eV for each additional carbon-oxygen bond. This separation is well within the resolution of modern instruments. Nevertheless, there are many cases where even carbon-oxygen species are not resolved into well-defined peaks or even shoulders: for example, nonspecific oxidation of organic materials can result in complex surface chemistries with many slightly different chemical structures and environments, which results in broad distributions of otherwise well-defined chemical shifts. In addition, secondary chemical shifts—which will be discussed in more detail below—tend to further broaden spectral envelopes. When applied to even more complex systems, e.g., materials that include both oxygen- and nitrogen-based functional groups, the above approach of including fit components for every expected functional group becomes quite difficult to justify. Functional groups such as amines (C–N bonds) and hydroxyls (C–O bonds) or carbonyls (C=O) and amides (N–C=O) give rise to peaks that are quite close in binding energy with separations of around 0.5 eV or less. The resulting excessive peak overlap, combined with the uncertainty in the exact peak energy for each component, means that the uncertainty associated with quantification is so great that the result of such an analysis is

no longer reliable or meaningful. In [Appendix D](#), we reproduce reference values of C 1s chemical shifts for a wide range of functional groups, taken from the most widely accepted and used database in the field of polymer XPS.<sup>10</sup>

## C. Differential charging

Differential charging refers to the nonuniform build-up of positive charge at and near a sample surface due to the emission of photo- and Auger electrons. Differential charging is a result of the inability of the charge compensation system to establish a uniform and stable potential across the whole sample and across all material phases (both in and out of the plane) during data acquisition. Differential charging is observed on many insulating materials, mixed electrically conductive and nonconductive materials, and materials electrically isolated from the spectrometer. The charge build-up in differential charging shifts the energies of photoelectrons emitted from a sample by an unknown amount, and because it is not necessarily uniform either across the sample surface or with depth, peak distortion is often observed. A problem occurs in the literature when authors do not recognize that their data are affected by differential charging, and they proceed to interpret spectral features that are simply artifacts of this phenomenon. A telltale sign of differential charging is for all the peaks in a survey scan to be distorted in the same way. This effect has been discussed comprehensively in two earlier guides of this series.<sup>1,11</sup> Differential charging can usually, but not always, be avoided by careful experimentation, including appropriate sample preparation and mounting techniques, optimization of instrumental parameters (especially, the charge compensation system), and customized data acquisition protocols. The reader is referred here to Stevie and co-workers' recent guide on sample handling and preparation in XPS.<sup>12</sup> Samples that are particularly susceptible to differential charging include insulating materials such as polymers, materials of large physical size and irregular shape, or mixed materials with conductive and nonconductive phases.

## D. Sample damage

While beam damage, including damage from photoelectrons, is often minimal in XPS under typical experimental conditions and data acquisition times, it does occur in some cases and should be monitored. For example, halogenated organic materials are often quite susceptible to beam damage. Without a test for sample damage, one cannot be certain that the spectra one obtains are truly representative of a material. A simple and important test for beam damage is to calculate the ratio of the survey spectra taken at the beginning and end of an analysis, where this ratio should obviously be unity. Some software packages save every narrow and survey scan collected and viewing these scans can reveal sample damage. Spectra from damaged materials may be fit to quantify/understand the damage. As an example of sample damage, see Patel and co-workers' report on poly(L-lactic) acid.<sup>13</sup>

## E. Incorrect assignments of chemical shifts

It is surprising how often one comes across published XPS spectra that have been curve-fitted using a number of shifted

component peaks that are then incorrectly assigned. A common example is a reversal of the labels for the C–O and C=O components. This mistake is all the more surprising because good, reliable XPS databases have existed for several decades.<sup>10,14</sup> What has to be kept in mind, of course, is that there is more to interpreting C 1s spectra than simply measuring the binding energy of a specific spectral feature and making assignments by looking up corresponding reference values in a database. Measured binding energies are often a mix of intrinsic (the sample chemistry) and extrinsic (associated with the XPS measurement, including interactions with x-rays, and secondary electrons, or flood gun electrons) effects.<sup>15</sup> As a consequence, reference values, which are usually measured on well-defined materials, may differ from the peak energies for the same chemical species on real-world samples.

### F. Consistency of curve-fit results

Any data processing and evaluation has to yield results that are internally consistent with the elemental composition determined on the same sample and/or consistent with prior knowledge about the material under question (theoretical structure/composition).<sup>9</sup> See, for example, Avval and co-workers' C 1s fit of gas phase CO<sub>2</sub> [obtained by near ambient pressure x-ray photoelectron spectroscopy (NAP-XPS)<sup>16</sup>], which is fit with just one synthetic peak (CO<sub>2</sub> only has one type of carbon), Patel and co-workers' fit of the C 1s spectrum of poly(L-lactic acid), which contains three peaks that correspond to the three chemical states of carbon, and Jain and co-workers' more complex C 1s fit of poly(γ-benzyl L-glutamate).<sup>13,17,18</sup> Examples of inconsistent results in the literature include cases where C 1s curve-fit assignments include specific functional groups even though the corresponding heteroatom is not detected in the survey spectrum. For example, in a recent publication, a component of the C 1s fit was assigned to C-Br even though no peak associated with Br was observed in the survey scan. Conversely, a published survey spectrum might clearly show the presence of a certain element, but this fact is ignored in the curve-fitting. Very commonly, Si is detected because Si contamination is ubiquitous in the human environment, e.g., polydimethylsiloxane (PDMS) is a very common contaminant on many surfaces. PDMS contamination will contribute to the C 1s signal due to its methyl groups, which has to be taken into account when analyzing the corresponding C 1s spectrum. This presence of surface contamination is, of course, an example where C 1s data may not be consistent with prior knowledge.

In addition, there should be consistency across the data obtained from different analytical techniques, although full agreement between methods should only be expected if the techniques probe the sample in exactly the same way. In general, developing a comprehensive understanding of surfaces requires the application of multiple techniques.<sup>19</sup> For example, XPS and time-of-flight secondary ion mass spectrometry (ToF-SIMS)<sup>20,21</sup> are nicely complementary in elucidating surface chemistry, where both are highly surface sensitive, probing the top few nanometers of surfaces. However, XPS is much more quantitative, and it provides direct information about the oxidation states of the elements. In contrast, ToF-SIMS often yields valuable molecular information that cannot be obtained by XPS, where the advantages of ToF-SIMS become

more apparent as the complexity of a surface increases. Another important surface sensitive technique is Auger electron spectroscopy (AES).<sup>22</sup> While AES typically does not provide as much chemical information as XPS, and the electron beam used to probe a surface may damage it, it offers extraordinary lateral resolution (10 nm) that should not be overlooked in material analysis. XPS data obtained via C 1s curve fitting often deviate significantly from corresponding data from other techniques that can probe much more deeply into materials, such as Fourier-transform infrared spectroscopy, Raman spectroscopy, x-ray diffraction, and spectroscopic ellipsometry.<sup>23–25</sup> In summary, the former surface sensitive methods (XPS, TOF-SIMS, and AES) restrict analysis to the upper few nanometers, which are often quite different from the bulk chemistry of a material that can be investigated by the latter techniques, which have typical sampling depths of hundreds of nanometers to several micrometers.

### G. Using/reporting adventitious carbon (AdC) for charge correction

By far, the most common method for correcting the BE scale for possible charging effects in XPS relies on the C 1s spectra of AdC present on essentially all surfaces exposed to the ambient air. As described in ISO and ASTM guides,<sup>26,27</sup> it is assumed that the C-C/C-H component of the measured C 1s spectrum of AdC will have a binding energy in the range of 284.6–285.0 eV. However, a scientist who is not aware of or willfully ignores the serious limitations and problems associated with using AdC as a peak energy reference could well be misled and end up misinterpreting XPS data. This topic has been discussed in more detail in another XPS guide of this series<sup>1</sup> and in other publications; for a historical perspective, see Greczynski and Hultman.<sup>28</sup> Briefly, the shortcomings of using AdC for charge correction include (1) the unclear chemical nature of AdC, which will not, in general, be the same from material to material, (2) the lack of a well-defined AdC peak energy value, (3) differences in the methodology of the BE scale correction, (4) the use of poor quality spectra as a result of differential charging, (5) the use of spectra with insufficient intensity to accurately identify the main peak, and (6) the lack of awareness when other, more reliable correction methods might be available. Nevertheless, we again emphasize that the use of a C 1s peak from a sample, including the AdC C 1s signal, is often a simple and useful method for charge correcting a spectrum to allow its other peaks to be identified and analyzed.

### H. Analysis of graphitic and mixed graphitic/nongraphitic materials

The analysis of graphitic, and especially mixed graphitic and nongraphitic, materials is often challenging, and unless care is taken, overfitting of the data can occur (see above). The importance of these materials, and the frequency with which they are analyzed in the literature, has increased greatly because of the discovery and subsequent interest over the last decades in novel graphitic nanomaterials that include Buckminster fullerenes, carbon nanotubes, graphene, and graphene oxide. There are unique aspects to fitting the C 1s spectra of graphitic structures, including their very characteristic C 1s peak shapes. It should be mentioned here that the

terms “graphitic” and “sp<sup>2</sup>-hybridized” as well as “nongraphitic” and “sp<sup>3</sup>-hybridized” are frequently used interchangeably in the literature. This is not correct because not all structures based on sp<sup>2</sup> carbon are graphitic in nature, such as being electrically conductive. Examples are vinyl groups and carbonyls.

More often than not, the study of graphitic materials, whether focusing on novel nanomaterials such as the ones mentioned above, or on more conventional ones such as carbon fibers (CFs) or activated carbon, involves the analysis of mixed systems that include both graphitic and nongraphitic forms of carbon. This adds another complicating aspect to what is, generally, already a rather complex and difficult challenge: the C 1s peak shape measured on graphitic structures is characteristically different from that originating from nongraphitic materials such as polymers and other organics. In the latter case, the peak shape can quite often be approximated as a symmetric, mixed Gaussian/Lorentzian line shape, which typically has very significant Gaussian character.<sup>29</sup> This approach is not possible for graphitic materials, where the presence of delocalized  $\pi$  orbitals leads to a small (or zero) bandgap. In the resulting metal-like systems, the carbon 1s spectrum will exhibit significant asymmetry toward higher binding energies due to the creation of low-energy electron-hole pairs, which screen the core hole and manifest as higher binding energy events.<sup>30,31</sup> See, for example, Jensen and co-workers' C 1s narrow scan of a forest of multiwalled carbon nanotubes.<sup>32</sup> Thus, one is faced with a combination of problems when attempting to analyze the C 1s region of advanced materials using curve-fitting. First, the “neutral” carbon peaks (C–C, C=C, C–H) of graphitic and nongraphitic carbon are typically only separated by about 0.4–0.6 eV, resulting in strong peak overlap, and second, the unique peak shape exhibited by graphitic structures cannot be simulated with a simple analytical function. Even an asymmetric, mixed Gaussian/Lorentzian function cannot always accurately represent this complex, irregular peak shape. Three peak shapes that might be considered here are a Voigt function, which is the convolution of a Gaussian and a Lorentzian, to which a decaying exponential tail is added,<sup>10</sup> and the asymmetric Lorentzian (LA) and finite Lorentzian (LF) peak shapes in CasaXPS,<sup>33,34</sup> which are Voigt-like peak shapes based on generalized Lorentzian functions that naturally allow asymmetry. The Doniach-Sunich (DS) line shape,<sup>35</sup> which was more frequently used in the past, has also been used for this purpose.<sup>36</sup> However, when there is any asymmetry in the DS line shape, it integrates to infinity, which is obviously problematic for quantitation. Problems with quantitation can also occur for LA line shapes with long tails (their integrals/areas will depend on where they are located in the peak envelope). This issue prompted the creation of the LF line shape, which has a parameter that suppresses the peak tail. Unfortunately, the literature increasingly contains attempts at fitting the complex spectra from graphitic and graphitic/nongraphitic materials using overly simplistic protocols, often without appropriate error analysis. For example, the C 1s of graphitic carbon is sometimes fit as a series of symmetric peaks for C–C/C–H and various carbon-oxygen containing functional groups, even when there is no oxygen (or insufficient oxygen, as shown in survey and narrow scans) to justify these assignments. In addition to these issues, the following problems are regularly observed in published C 1s peak fits (a more complete version of this list has been previously published):<sup>2,37</sup> scan windows that are too narrow, not

showing the original data, fitting data that are too noisy, labeling noise as chemical states, using a wide range of peak widths without justification, an inappropriate baseline, incorrect synthetic line shapes, and improperly comparing different, related spectra.

Finally, in many cases, these problems do not occur in isolation, but rather in combination with each other. For example, one may find that raw spectra that are obviously distorted by *differential charging*, have been *incorrectly charge-corrected*, then *overfitted* using a *simplistic curve-fit protocol*, and finally quantified *without any error analysis*. Needless to say, this type of analysis only adds to the growing body of irreproducible results.

### III. CURVE-FITTING CARBON

The overwhelming majority of published errors relate to curve-fitting. In this section, we will provide a brief introduction to this important data processing method, including general rules and tips based on best practices. Importantly, this is not intended to be a comprehensive treatment of the topic; for more detailed and in-depth discussions, we refer to previously published guides that either cover curve-fitting in general or specific aspects of the method.<sup>37–44</sup>

The objective of fitting XP spectra with a set of components is to enable the identification and quantification of individual spectral peaks. These can then be assigned to specific chemically/physically significant entities so that material proportions and/or properties can be inferred. This process is often described as deconvolution in the literature, which is incorrect.<sup>45,46</sup> In XPS, the original photoelectron peak is broadened as a result of convolutions with functions attributable to all the processes affecting the photoelectrons as they travel to the detector and are detected. Deconvolution is the mathematical process of removing these broadening functions to reveal the original narrow line shape. By contrast, curve-fitting involves generating a synthetic spectrum by adding several individual component peaks with the objective of simulating the experimental spectrum with the synthetic spectrum. The latter process does not modify the experimental spectrum, whereas the former does. Quantities of significance in XP peak fitting include the binding energy (BE), peak width (full width at half maximum or FWHM), peak shape, and peak area of synthetic fit components. Once identified and correctly assigned, the position of a component peak may be used for charge correction. Peak positions also provide the basis for assigning peaks to both elements and chemical environments. The FWHM can be an indicator of chemical environment, as too are peak shapes that vary from simple symmetric narrow peak shapes to complex structures characteristic of the electronic structure and oxidation state of the material. The amount of substance (atomic concentration) is determined by measuring relative peak areas, which requires the separation of zero energy-loss signals—the actual core line plus associated features—from the inelastically scattered background.

The art of fitting data with peaks consists of selecting the appropriate number of component peaks, using appropriate synthetic line shapes, and limiting the set of fitting parameters through relationships (constraints) to produce peak models capable of determining physically meaningful quantities from XPS spectral forms. Note that we use the term “art” in the sense of “a skill

acquired as the result of learning and practice.” It requires years of study and practice to become skilled in this art form, but the good news is that everyone with a basic science training and a good understanding of physics, mathematics, and chemistry can achieve proficiency. We cannot emphasize enough how important the analyst is in guiding the fitting process. One cannot rely on software and algorithms to produce reliable and meaningful results, although there are ongoing efforts to produce expert systems (now through artificial intelligence) that may be able to at least catch some of the common errors made in XPS peak fitting.<sup>47,48</sup> The so-called chi-by-eye approach to fitting,<sup>49</sup> which refers, somewhat humorously, to the skilled analyst’s ability to rapidly assess the quality of a peak fit by visual inspection, is, in a sense, both the simplest and most advanced method of evaluating XPS peak fits. The novice’s approach is to accept the results of analysis software without questioning their validity, i.e., if the sum of the fit components matches the data envelope, the fit must be good. The more advanced approach (chi-by-eye of the expert) is to ask whether the results make good chemical and physical sense in the context of all the information available about the problem, including the analyst’s experience. Ultimately, it is the analyst who imposes meaning based on a thorough understanding of instrument technology, mathematics, and materials science.

The actual procedure for fitting component peaks to spectra uses mathematical algorithms to minimize a figure of merit; the latter being a measure of how closely the mathematical model fits the experimental data. The algorithm generates a sequence of increments in fitting parameters leading from the initial state to a final state that represents a minimum with respect to the figure of merit. Importantly, this figure of merit, typically chi square or the residual standard deviation (see examples<sup>13,17,50,51</sup>), is a single number used to guide adjustments to potentially numerous fitting parameters, possibly generating numerous paths leading to potentially numerous outcomes. That is, the fit may not be unique—the analyst should be aware of the possibilities of fit parameter correlation and/or that the fitting algorithm may land in a local, but not a global, minimum.<sup>43</sup> Please note that the authors of this guide use a specific data processing software package (CasaXPS; Casa Software Ltd, UK) and we will, at times, refer to this application and the various options and features available in it. However, the methods described and the advice provided here are generally applicable.

### A. Steps in fitting high resolution C 1s spectra

Some of the topics that will be discussed below have been covered in the recent series of guides on XPS in the *Journal of Vacuum Science and Technology*.<sup>8</sup> They are brought up again in this section with specific reference to certain aspects of C 1s peak fitting because they are central to the analysis of C 1s spectra.

1. Every XPS experiment begins with asking relevant questions:
  - a. What is the information required? What is the objective of the analysis?
  - b. What additional data (spectra) need to be acquired to enable optimal analysis of the C 1s region? A wide scan (survey spectrum) should always be taken of a material, plus any other relevant narrow/detail scans, depending on what elements and functional groups are expected. For more information on

survey spectra, see Shah and co-workers’ guide on this topic.<sup>52</sup> The survey spectrum may reveal the presence of unexpected elements on a surface, which may influence the C 1s analysis. Surface analysis is full of surprises! Data from other surface and bulk analytical techniques may also shed light on the material in question.

- c. What is the best compromise between all the different experimental acquisition parameters to achieve optimum data quality, i.e., high S/N, good resolution, uniform and stable charge compensation, minimum sample degradation due to X-radiation? XPS data acquisition is discussed in greater detail in Major and co-workers’ guide to peak fitting.<sup>37</sup>
2. Once the data are acquired, they should not be processed in any way prior to curve-fitting to avoid introduction of artifacts. For example, smoothing the data changes its underlying frequency components.<sup>46,53</sup>
3. Starting with all the relevant information available at this point, including data from other characterization techniques, construct an initial fitting model. A peak model is defined in terms of component peaks and a background algorithm. These in turn are specified using synthetic line shapes, a range of fitting-parameters, and, for the most part, one of a few specific backgrounds. XPS peak fitting, in general, is discussed in Major and co-workers’ guide on this topic.<sup>37</sup> XPS backgrounds are covered in Engelhard and co-workers’ guide on this topic.<sup>54</sup> Tougaard adds important insight into XPS background analysis in his guide to the analysis of complex (nonhomogeneous) samples.<sup>55</sup> See also Major and co-workers’ guide on the LX type line shapes, i.e., LA, LF, and LS, which are increasingly used in XPS peak fitting.<sup>56–59</sup>
4. After each iteration of the optimization process, all component peaks are summed with the background shape to form an approximation to the overall spectral envelope. Importantly, no background or line shape is fully correct. Most analyses are based on practical models that are acceptable approximations. Take into account the following:
  - (a) The chemical functionalities to be expected, which are based both on what is known about the sample and also on whatever the survey spectrum has revealed to be on the surface. As noted above, (1) the series corresponding to C–C/C–H, C–O, C=O/O–C–O, carboxyl/ester, and carbonate fit components shows up in the analysis of many organic materials (even materials formed entirely from carbon, or carbon and hydrogen, often show some oxidation), and (2) the synthetic peak shapes needed for an analysis vary depending on the type of carbon present in the sample. One of the most important contributions to the XPS analysis of organic materials, and arguably to XPS in general, was Beamson and Briggs’ book on *High Resolution XPS of Organic Polymers*.<sup>10</sup> In their book/database, they show carefully collected spectra of high-quality polymer specimens. Polymers containing carbon, oxygen, and hydrogen are the largest group of polymers covered in their database. However, they also provide spectra of hydrocarbon polymers, as well as those containing nitrogen, fluorine, chlorine, sulfur, and silicon (see [Appendix D](#): Primary

and secondary C 1s chemical shifts). The reader is also referred to the *Surface Science Spectra* database for more XPS spectra of organic materials, as well as to Easton and co-workers' guide on the XPS analysis of polymers.<sup>11,60</sup>

- (b) Because of the importance of graphitic materials in materials science today, analysts must be aware of the possibility of shake-up peaks in their C 1s spectra. For example, in their guide on the XPS of catalysts, Davies and Morgan showed an example of a catalyst containing graphitic carbon with its typical shape, i.e., a tailing C 1s signal and a shake-up signal.<sup>61</sup> Shake-up peaks, which are also known as shake-up satellites, are due to  $\pi \rightarrow \pi^*$  type transitions in which electrons in highest occupied molecular orbitals (notice that orbitals is plural here) are promoted to lowest unoccupied molecular orbitals in molecules and materials. Here are a few highlights from Beamsom and Briggs' book that may be helpful.<sup>10</sup> Polymers containing carbon-carbon double bonds like butadiene show small shake-up peaks, and polymers like polystyrene with aromatic (phenyl) rings show somewhat larger shake-up signals that are centered around 6–7 eV above the main carbon peak and are generally quite broad, often extending to even higher energies. As a conjugated aromatic structure increases in size, its shake-up signals become more complex and some of them occur at lower binding energy. Shake-up signals take intensity from the main peak(s) in a peak fit and should be included in quantitation. Both Shard<sup>62</sup> and Brundley and Crist<sup>63</sup> have discussed shake-up signals in their guides on XPS quantitation. With the exception of polystyrene, which shows a shake-up structure that is very similar to gas phase benzene, Beamsom and Briggs' fits to shake-up peaks did not have physical meaning. The implication here is that the measurement of analogous molecular systems, perhaps by NAP-XPS, and/or first principle calculations might be valuable in assigning and understanding shake-up signals. Note that a common error in C 1s peak fitting is for authors to fit and assign shake-up signals as chemically shifted peaks. Shake-up peaks are also discussed in Major *et al.*'s guide to peak fitting.<sup>37</sup>
- (c) Other elements that have potentially overlapping peaks in the C 1s spectral region. Ruthenium, in particular, will add considerable complexity. The Ru 3d doublet overlaps with the C 1s signal, and it needs very careful analysis and a sophisticated fitting protocol if the contributions from C and Ru are to be correctly identified and quantified.<sup>41</sup> The K 2p signal is also moderately close to the C 1s envelope. As a result, a small K 2p<sub>3/2</sub> signal may be confused for a C 1s shake-up peak or the K 2p doublet may be confused with the C 1s doublet feature that is typically observed for perfluoropolyethers (e.g., O—CF<sub>3</sub> and O—CF<sub>2</sub>—O).
- (d) Prior knowledge about instrument performance and how data are affected by different instrumental parameters. It is assumed, of course, that the instrument is in optimum working order, fully calibrated, and that instrumental performance is regularly checked by the operator. The reader here is directed to Wolstenholme's guide on rapidly assessing the performance of an XPS instrument.<sup>64</sup>
- (e) The spectral envelope (raw data). Identify any spectral features that would help in guiding the construction of an initial model: clearly resolved peaks, shoulders, asymmetries, peak widths, and anything else that might suggest the presence of an additional component peak. Even weak features such as shake-up structures, etc., provide useful information. See, for example, Avval and co-workers' C 1s fit of polyethylene terephthalate, which includes fitting of the shake-up signal.<sup>65</sup> A good peak fit/analysis should be consistent with all the information in a spectrum and other information about a sample.
- (f) Start with as few component peaks as possible. Additional components can be added during later iterations.
- (g) Secondary chemical shifts are experienced by C atoms adjacent to one experiencing a primary chemical shift, i.e., secondary shifts occur on C atoms that have no direct bond with the heteroatom(s) on the primarily shifted carbon. Consequently, secondary shifts are usually small, typically well below 1 eV. A common example of a secondary shift, which is fairly strong, is in the methylene (CH<sub>2</sub>) group next to the ester carbon (C(O)—OR) in a fat/oil, i.e., CH<sub>2</sub>C(O)—OR. That is, the strong withdrawal of electrons by the three C—O bonds around the ester carbon leads to noticeable electron withdrawal from the neighboring CH<sub>2</sub> group. Often, secondary shifts cause an apparent asymmetry of the main (unshifted) hydrocarbon peak (this peak does not actually become asymmetric, rather it is the presence of multiple chemical states that are chemically shifted by small amounts that effectively induces it), but they may also appear, albeit rarely, as well-resolved spectral features. In whichever case, these secondary chemical shifts need to be accounted for in C 1s curve-fitting in some form:
- (i) In some cases, secondarily shifted peaks are reasonably well-defined, such as in acrylic polymers. As just noted, the strongly shifted ester carbon (primary shift of ~4 eV) creates a secondarily shifted carbon (~0.6–0.7 eV shift) that can often be identified and included in the fit model as a separate component with appropriate constraints (peak area fixed to the ester peak). Examples of secondarily shifted peaks included as separate components in C 1s fits include Avval and co-workers<sup>65</sup> and Roychowdhury and co-workers<sup>66</sup> fits of the NAP-XPS spectra of polyethylene terephthalate and Italian cheese, respectively.
- (ii) In cases where a range of functional groups with a range of secondary shifts cause ill-defined broadening on the high BE side of the unshifted carbon peak (C—C/C—H),<sup>67</sup> one can either account for this peak asymmetry by using an asymmetric line shape for the main peak or by including a minor second peak just above the main peak. For whichever solution chosen, the analyst needs to be aware that any quantitative results obtained from this spectral region by such a fit will be associated with considerable uncertainty, including for any component peaks due to C—N and C—O based functional groups and the like.
- (h) Choose the most appropriate background and line shapes. Some variation of a Tougaard-type background would be



most realistic, e.g., the three-parameter universal Tougaard background “U 3 Tougaard” (as offered in CasaXPS), or a Universal Polymer Tougaard background (also offered in CasaXPS). As an example of the latter, see Patel and co-workers’ peak fitting of the NAP-XPS C 1s spectrum of poly(L-lactic-acid) and Jain and co-workers’ C 1s peak fitting of poly( $\gamma$ -benzyl L-glutamate).<sup>13,18</sup> Sometimes a Shirley-type background is an acceptable approximation; if there is little or no rise in the baseline, it will make little difference whether a Shirley or a linear background is used.<sup>66</sup> However, Shirley backgrounds are not, in general, recommended for insulating materials because of their wide bandgaps. In cases where there is no rise in the baseline (see, for example, the C 1s spectra of gaseous CO<sub>2</sub> and polycyclohexene by NAP-XPS<sup>17,50</sup>), a linear background is often appropriate. Recommended synthetic line shapes typically combine characteristics of both Gaussian and Lorentzian functions (through addition, multiplication, or convolution) with an option to introduce asymmetry. As noted above, examples of the latter include the Voigt function with an exponential tail, and the generalized Lorentzian function with optional asymmetry, e.g., the asymmetric Lorentzian (LA)<sup>33</sup> and finite Lorentzian (LF)<sup>34</sup> line shapes in CasaXPS. For example, the C 1s spectra of CO<sub>2</sub> and polycyclohexene just discussed are better fit with asymmetric LA line shapes than with symmetric Gaussian–Lorentzian sum or product functions.<sup>17,50,68</sup> The LA and LF, i.e., LX, line shapes are discussed in Major and co-workers’ guide on this topic.<sup>56</sup>

- (i) A very useful option is the use of experimental spectra as peak fit components instead of analytical functions. As mentioned above, graphitic carbon gives rise to complex peak shapes that cannot be easily approximated with analytical functions. Having a reference spectrum of the pure graphitic material allows one to use it as a fit component and thus ensure that the graphitic component of the spectrum is quantified correctly within usual limitations and uncertainties. Using reference spectra as fit components can also be very useful in cases where samples are mixtures of distinctly different materials.<sup>11</sup> If reference spectra of the individual, pure constituents are available, and if it can be assumed that those constituents remain chemically/physically unchanged in the mix, using their respective reference spectra can simplify peak fitting significantly. This approach also applies to the analyses of thin coatings where signals from both the substrate and the coating can be detected. In those cases, it might be sufficient to construct a simple two-component model using experimental reference spectra of the uncoated substrate and pure coating.
  - (j) For complex materials, it may be worthwhile to perform first principles (quantum) calculations on the molecules/systems under analysis.<sup>69,70</sup> Such calculations can be useful in predicting, ordering, and comparing the energies of peaks from different functional groups. See, for example, the C 1s fits of polyethylene terephthalate and poly( $\gamma$ -benzyl L-glutamate) (PBLG).<sup>18,65</sup> Unfortunately, we are not aware of any *ab initio* system or approach that can fully calculate narrow scans or replace the traditional approach outlined here.
5. Apply any initial constraints to fit parameters that can be justified based on prior information. For example, it is often reasonable to constrain the FWHM of all component peaks to a similar value, i. e., to within  $\pm 0.1$  or  $0.2$  eV. If a C 1s spectrum has an isolated component, its width can be used as a standard for the other components. In complex, multicomponent fits, it is often best to constrain all fit components to have the same width, e.g., see Jain and co-workers’ C 1s fits of PBLG.<sup>16</sup> On modern instruments using monochromated Al K $\alpha$  radiation under typical high-resolution conditions, one can realistically expect FWHM values of  $0.8$ – $1.4$  eV on organic (nonconductive) materials. In the case of reference spectra used as fit components, the “peak width” needs to be fixed to the original value and should not vary.
  6. Perform the first optimization of the model using a minimization algorithm.
  7. Make appropriate adjustments to the peak fit model based on the results of the first iteration. This might include adding/removing/adjusting peak components and/or constraints. Two criteria have to be met simultaneously:
    - (a) It is obviously important to obtain a mathematically good fit to the experimental spectrum, checking the figure of merit and the residuals across the whole spectrum. Ideally, the residuals will not show any structure, i.e., they will appear as random noise. In the case that they do show structure, they often point to imperfections or inadequacies in the peak fitting that may need to be addressed. See, for example, Avval and co-workers’ fit of the NAP-XPS C 1s spectrum of gas phase CO<sub>2</sub>. Here, a fair amount of structure was evident in the residuals of the fit when a symmetric Gaussian–Lorentzian sum function was employed, but this structure was reduced when a line shape with some asymmetry was used, suggesting that this fit better matched the chemistry and physics of the sample and instrument.<sup>17</sup>
    - (b) It is equally important to ensure that the quantitative values generated by the fit (peak positions, widths, areas) are realistic, physically meaningful, and are consistent with what can be reasonably expected based on all the available information about the material under study. This includes the elemental composition obtained via survey spectra. At this point, the expertise and experience of the analyst count significantly. Because of the complexity of peak fitting, it is easy to overlook one of the multiple factors influencing the overall shape of an XP peak fit. When in doubt, consult with more experienced colleagues for help and advice.
  8. Repeat the last two steps until the above two criteria are met and no further significant improvements are possible. The emphasis here is on “significant improvements.” For example, spending a lot of time tweaking line shapes simply to reduce the figure of merit by a tiny fraction, especially when the figure of merit you are using is already in a low and acceptable range and the residuals show little or no structure, is probably not a good use of time.
  9. In general, when noticeable artifacts are present in spectra due to extensive differential charging, it may not make sense to peak fit the distorted spectra. In these cases, it may be better to evaluate overall peak shapes and widths using a width function.<sup>71</sup> For example, Jain *et al.* utilized the equivalent width to

follow the peak width/shape of the F 1s signal from polytetrafluoroethylene as a function of background gas pressure in NAP-XPS, where the peak became increasingly broad and distorted with decreasing pressure.<sup>72</sup> Surface charging is discussed in Baer and co-workers' guide on this topic.<sup>1</sup>

10. Various informatics/chemometric methods, such as principal component analysis (PCA) and multivariate curve resolution (MCR), can be helpful for comparing whole spectra to each other and identifying the differences between them. These differences may point to chemical state differences that may aid in peak fitting. For example, a recent study by Chatterjee and co-workers showed PCA and MCR analyses of XPS depth profiles through silicon dioxide on silicon via series of Si 2p and O 1s narrow scans and tantalum oxide on tantalum via series of Ta 4f and O 1s narrow scans.<sup>73</sup>
11. Finally, be aware of the errors and uncertainties associated with peak fitting when interpreting and reporting results. Comprehensive error analysis in peak fitting is not trivial, which is probably one of the reasons why it is rarely published in the general materials science literature. Without error analysis, however, the reader cannot assess the significance and/or reliability of the reported results and interpretations. A common method for estimating errors in XPS is based on some form of Monte Carlo analysis. Instead of repeating an experiment many times which is not always practical, estimates for uncertainties in the peak parameters are being made using assumptions about the noise typical of XPS spectra. The essence of Monte Carlo methods for estimating uncertainties is to take a dataset, remove the noise from the data, then repeatedly add noise to the synthesized data to generate a set of simulated experimental results, and apply the chosen peak fit model to those artificial data. The results represent a distribution for each of the parameters from which an error matrix and tabulated parameter distributions can be extracted. The distribution of the calculated quantity shows the effects of the imprecision of the fit parameter, and also how strongly different parameters are correlated. Another approach along these lines is to consider generating a uniqueness plot<sup>43,74</sup> to confirm that fit parameter correlation is not taking place when a fairly large number of fit parameters is used. Fit parameter correlation diminishes the statistical validity of a model. The literature now contains various examples of uniqueness plots in C 1s peak fitting.<sup>13,40,51,66,75</sup> Finally, we note an approach that is reminiscent of the "disproof by counterexample" method in mathematics in which a mathematical statement can be shown to be false by just one single counterexample. In this approach, which is discussed and employed in [Appendix C](#) below, a fit is initiated from two or more different starting points. If the fit converges to the same solution, it may be a good fit. However, if the different starting points, e.g., different initial areas of the synthetic peaks in the fit, cause it to fall into very different local minima, the protocol is questionable and perhaps flawed. All three of these methods, Monte Carlo analysis, uniqueness plots, and "disproof by counterexample" can be performed in CasaXPS (the disproof by counterexample approach is not automated—one has to choose noticeably different, but still reasonable, starting conditions for the fits). Of course, it is not practical, nor would we recommend, that an

error analysis be performed for every peak fit. However, at the very least, such an analysis should be carried out whenever a new peak fit model is constructed for a new class of materials to assess the robustness of the model and the confidence limits associated with the resulting quantitative values.

#### IV. SUMMARY AND CONCLUSIONS

The carbon 1s photoelectron spectrum is the most widely analyzed XPS signal in the materials science literature, but, alarmingly, the proportion of publications showing flawed and erroneous analyses is high. XP peak fitting is a processing technique that is often employed inappropriately and incorrectly, leading to unreliable and irreproducible results and, ultimately, to invalid conclusions. The most common problem areas here result from overfitting, i.e., including too many fit components in a fit when they are not justified, not placing appropriate constraints on fit components, a lack of appropriate error analysis, using inappropriate peak shapes and backgrounds, differential charging, incorrect assignments of chemical shifts, ignoring other information about the sample (e.g., information in the survey spectrum or information about the material's structure), inappropriately using and reporting adventitious carbon for charge correction, and incorrect analysis of mixed graphitic/nongraphitic materials. Many different types of minor errors can also be identified. In the opinion of the authors, most errors in the literature are due to a lack of expertise and experience of the XPS analyst.

This present guide forms part of a series published as a Special Topic Collection by the *Journal of Vacuum Science and Technology A*, entitled "Reproducibility challenges and solutions." The objective of this Special Topic Collection is to provide educational tools for both inexperienced and more experienced surface scientists to improve and develop their expertise in all aspects of the XPS analysis. To that end, we have provided here a step-by-step guide to C 1s narrow scan analysis in general and to C 1s peak fitting in particular. We propose that by following these protocols, one can cover the relevant aspects of the C 1s analysis and ensure that key factors that might potentially affect the data are taken into account.

Finally, we include in the appendix several examples that illustrate the more common problems encountered in the literature and ways of correctly analyzing C 1s spectra, based on the rules and guidelines outlined in this document.

#### ACKNOWLEDGMENTS

The authors would like to thank Paul Pasic and Helmut Thissen who assisted in reviewing the manuscript prior to submission. M.R.L. and G.H.M. acknowledge the Department of Chemistry and Biochemistry and the College of Physical and Mathematical Sciences at Brigham Young University for their support of this research. C.D.E. and T.R.G. acknowledge CSIRO Manufacturing for supporting this work.

#### Nomenclature

AA	= Acrylic acid
AdC	= Adventitious carbon

amu	= Atomic mass units
ASTM	= ASTM International, formerly known as American Society for Testing and Materials
at. %	= Atomic concentration
BE	= Binding energy
CF	= Carbon fiber
CVD	= Chemical vapor deposition
eV	= Electron volt
FWHM	= Full width at half maximum
g/mol	= grams per mole
GO (rGO)	= Graphene oxide (reduced graphene oxide)
HOPG	= Highly oriented pyrolytic graphite
ISO	= International Organization for Standardization
M	= molar (mol/l)
MCR	= Multivariate curve resolution
NAP-XPS	= Near-ambient pressure XPS
NIST	= National Institute of Standards and Technology
PCA	= Principal component analysis
PDMS	= Polydimethylsiloxane
STD	= Standard deviation
S/N	= Signal-to-noise ratio
ToF-SIMS	= Time-of-flight secondary ion mass spectrometry
U 3 Tougaard	= Universal 3 parameter Tougaard background shape. The energy loss cross section defining this background is customizable using three adjustable parameters.
XPS	= X-ray photoelectron spectroscopy

## APPENDIX A: OVERFITTING, “APPROPRIATE” FITTING, AND FITTING WITH MODEL SPECTRA

In this example, we describe the analysis of a moderately complex organic material. Curve-fitting the C 1s is challenging, and it is tempting to overfit the spectrum, i.e., use more component peaks than could be reasonably justified, based on what we know and expect about the material under study. We present two fit protocols, the first one representing overfitting and the second one based on the guidelines outlined in the main text (Sec. III). We then employ the basic error analysis to compare these two fit protocols. Finally, we demonstrate that by using experimental spectra of reference compounds as fit components, both the analysis and the interpretation can be simplified significantly.

### Background

Inhalable drugs may absorb atmospheric moisture, causing powder aggregation and adversely affecting powder dispersion and deposition in the lung. The following experiment was part of a study exploring the use of hydrophobic amino acids (valine among others) for protection against moisture in spray-dried amorphous powders. Disodium cromoglycate (DSCG) was used as a model drug, the latter being an anti-inflammatory medication used to treat asthma.<sup>51</sup> The structures of the two compounds are shown in Fig. 1.

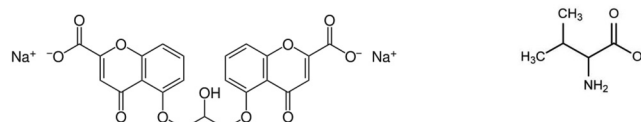


**FIG. 1.** Structures of DSCG (5-[3-(2-Carboxylato-4-oxochromen-5-yl)oxy]-2-hydroxypropoxy]-4-oxochromene-2-carboxylate disodium salt) and valine (2-Amino-3-methylbutanoic acid).

### Analysis

Five samples with different ratios of the two constituents were available for analysis (Table I).

The two pure compounds were included as reference compounds (Samples #1 and #5). The objective of the analysis was to determine the surface compositions of the samples and, if possible, estimate relative molar fractions of each constituent on the surface of the powder particles. Here, we will focus on the analysis of the C 1s high resolution spectra. Figure 2 shows the C 1s spectra of the three mixed samples and of the two pure compounds. A systematic change in the spectral envelope as a function of the changing molar ratio can easily be observed. The corresponding survey spectra (not shown) revealed the presence of only C, O, N, and Na, as expected, which in the case of the two reference samples were in approximately the expected concentrations. This indicates that no significant and detectable contaminants were present.

The first and obvious step here would be to fit the two reference spectra to confirm the structures of the two compounds and to determine chemical shifts for the various peak components corresponding to functional groups in the structures. Here, we use a slightly modified Universal Polymer Tougaard background and pseudo-Voigt functions (LF line shapes in CasaXPS) for the component peaks, slightly asymmetric where appropriate, e.g., in the case of the main CH<sub>x</sub> component to account for secondary chemical shifts. The peak width of components is constrained to a narrow range of 1–1.4 eV except for the two peaks used to fit the shake-up signal of DSCG. The fits are quite straightforward as shown in Fig. 3. In the case of DSCG, we use four components at 284.7 eV (CH<sub>x</sub>), 286.74 eV (C–O), 287.7 eV (C=O), and 288.61 eV (O–C=O). The extended feature between 290 and 294 eV (aromatic shake-up) is fitted with two additional broad peaks. The spectrum of valine is fitted with three peaks at 285.0 eV (CH<sub>x</sub>), 286.22 eV (C–N), and 288.24 eV (O–C=O). The reference BE values for aromatic and aliphatic CH<sub>x</sub> were taken from the Polymer XPS Database

**TABLE I.** List of samples included in the analysis.

	DSCG (mol. %)	Valine (mol. %)
#1	100	0
#2	67	33
#3	48	52
#4	26	74
#5	0	100

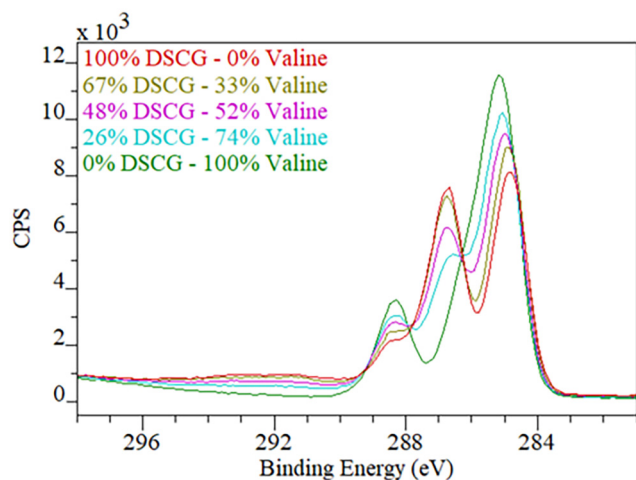


**FIG. 2.** C 1s high resolution spectra of five DSCG-Valine mixtures. CPS is photoelectron counts in counts/s.

by Beamson and Briggs.<sup>11</sup> Note that the rather low BE value for the acid peak in the case of valine most likely indicates that the acid is in the deprotonated form ( $^-O-C=O$ ); consistent with this possibility, the position of the N 1s peak (401.4 eV) suggests the amine group is protonated ( $NH_3^+$ ; not shown). Importantly, the measured peak positions as well as the relative concentrations obtained for the curve-fits confirm that both reference compounds have the expected structure and stoichiometry.

Having successfully fitted the two pure compounds and having established peak positions for each functional group present in the two constituents, one might be tempted to simply transfer the combined fit model to the spectra of the three mixed samples. This would mean using one component peak for each functional group identified in the two reference spectra, i.e., nine peaks in total. An

example of this is shown in Fig. 4(a) with the corresponding component labels and positions listed in Table II (left column). At this point, it would be worth pausing and asking oneself a few questions based on the step-by-step guidelines outlined in the main text:

**Q:** Is there significant peak overlap between any two adjacent components?

**A:** Yes, there are several cases with components being separated by 0.5 eV or less. These pairs of components will be highly correlated and their relative peak areas extremely sensitive to positions.

**Q:** How precisely can we measure peak positions in this case?

**A:** Even with careful experimentation using a well-calibrated instrument, one could expect the uncertainty to be  $\pm 0.2$  eV at best, but likely worse.

**Q:** How certain are we that the two different compounds, DSCG and valine, do not react or are otherwise affected chemically/physically when being mixed?

**A:** We can't be certain, although their chemistry suggests they will not react directly with each other. However, to be safe, we must allow for the possibility that mixing might affect the types of functional groups present or their respective peak positions. We should also remember that even if no reaction takes place between two materials, most materials have different surface energies/tensions, which often leads to one of the components (the one with the lower surface energy/tension, i.e., the more hydrophobic one or the one with the most hydrophobic group) preferentially occupying the outermost surface of a material. Such preferential positioning can affect XPS signals.

**Q:** How certain are we that the effects of differential charging on the spectra of the two compounds are the same in a mixed sample as in the two pure compounds?

**A:** We can't be certain. It may depend, for example, on the morphology of the mixed material and/or on whether the two compounds were affected chemically/physically when being mixed.

Additional questions could probably be asked. Suffice it to say that the overall uncertainty resulting from all those unknowns would render any results derived from such a fit (with nine components) unreliable, and subsequent conclusions meaningless. Such a fit

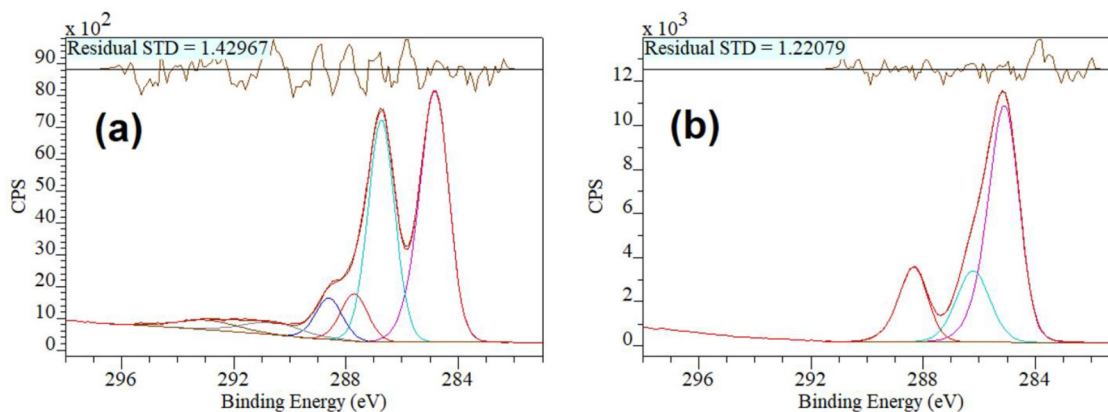


**FIG. 3.** Fitted C 1s spectra of pure reference compounds: (a) DSCG and (b) Valine. CPS is photoelectron counts in counts/s.

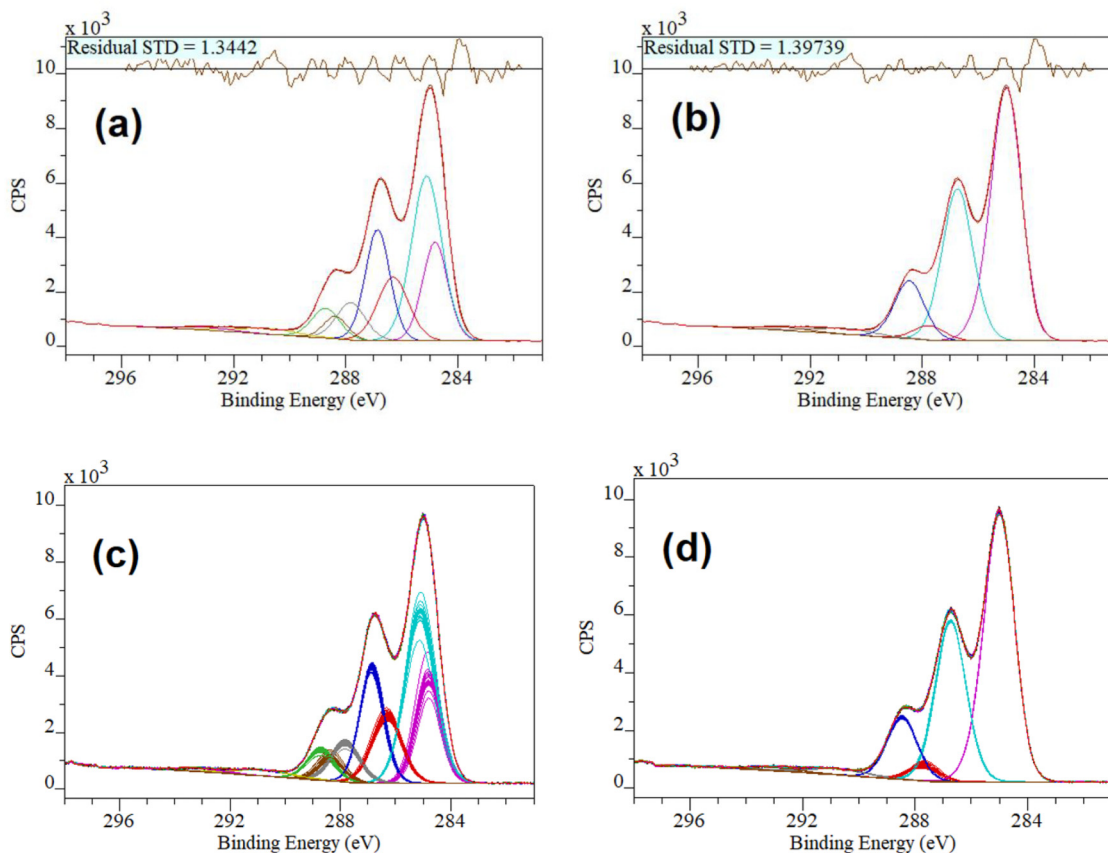


**FIG. 4.** C 1s spectrum of a mixed sample (48 mol. % DSCG-52 mol. % valine) with two different fit models applied, both using synthetic line shapes: overfitted spectrum (a) vs recommended fit (b). (c) and (d) show the results of Monte Carlo based tests of these two peak fit models (see text for details). CPS is photoelectron counts in counts/s.

protocol should therefore be rejected. Instead, the number of fit components should be reduced. In those cases where two functional groups give rise to peaks being very close together, one single component peak should be used. This single component would account for both functionalities together. For example, the peaks due to aromatic and aliphatic  $\text{CH}_x$  should be combined in one component peak. In Table II, we list the resulting six components (column on the right). An actual fit based on this recommended protocol is shown in Fig. 4(b). Note that according to the residuals and the figure of merit (Residual STD), the latter fit is only slightly worse (mathematically speaking) than the overfitted example. To test how reliable the different fit models are in determining important peak parameters such as peak area (which would subsequently be converted to atomic concentrations), we apply a simple Monte Carlo based method as described in the main text. Figures 4(c) and 4(d) display overlay plots of all the simulated experimental spectra generated by a Monte Carlo analysis, fitted according to the two different fit models. In the case of the overfitted spectra [Fig. 4(c)], we observe a great deal of variation in the peak heights. For example, the peak area for C1

(284.7 eV) varies by 33% and that of C2 (285.0 eV) by 67%. This is not surprising since those two components are strongly correlated. In the case of the recommended (simplified) peak model, the area of the combined component peak (C1 + C2) only varies by 1%. This confirms our decision to reject the first peak fit model.

Of course, it would be difficult to determine surface fractions of DSCG and valine, even in the case of the “recommended” fit. However, this could potentially be achieved by comparing the elemental compositions of the mixed samples with those of the two reference compounds. This would be quite reliable in this case because valine is characterized by having a unique element (nitrogen). In general, one should always be aware of, and accept, the limitations of XPS as an experimental technique instead of pushing it beyond its limit, for example, by overfitting.

An alternative method for identifying fit parameter correlation is based on uniqueness plots. A uniqueness plot for a peak fit is created by systematically changing one of the parameters in the fit, while allowing all other parameters to vary as they did in the original fit. Each time the designated fit parameter is changed and fixed at its

**TABLE II.** Comparison of the first two curve-fit protocols described in the text for a mixture of DSCG and valine [see Figs. 4(a) and 4(b)].

Overfitted			Recommended fit	
C 1s component	Position (eV)	Assignment	Position (eV)	C 1s component
C1	284.7	CH <sub>x</sub> (aromatic - DSCG)	284.9	C1 + C2
C2	285.0	CH <sub>x</sub> (aliphatic - valine)		
C3	286.2	C–N (valine)	286.7	C3 + C4
C4	286.7	C–O (DSCG)		
C5	287.7	C=O (DSCG)	287.8	C5
C6	288.2	O–C=O (valine)	288.5	C6 + C7
C7	288.6	O–C=O (DSCG)		
C8	290.8	Aromatic shake-up (DSCG)	290.8	C8
C9	293.1	Aromatic shake-up (DSCG)	293.1	C9

new position, the fit is repeated, and the figure of merit is recorded. A uniqueness plot is the plot of the figure of merit (for example, the residual STD) as a function of the value of the varied (and fixed) fit parameter. Three uniqueness plots (see Fig. 5) were generated for the fits in Figs. 4(a) and 4(b). The uniqueness plot created for the synthetic peak (C5) at 287.8 eV in Fig. 4(a) (the black trace in Fig. 5) is nearly a horizontal line, which indicates that there is little uniqueness for this fit component, i.e., the position of this peak can be varied to a very significant extent without the overall error changing to any substantial degree. Thus, at any position defined for this peak, the other parameters can be varied to compensate for its new position—the position of this peak has no statistical significance and the fit parameters are correlated. *A priori*, one might have expected that there would be fit parameter correlation for the fit presented in Fig. 4(a) because of the large number of components. The red trace in Fig. 5 corresponds to the uniqueness plot for the synthetic peak (C5) at 287.8 eV in Fig. 4(b). This plot shows that there is a range of positions for the peak in which there is only a small rise in the error of the fit, again indicating some fit parameter correlation. This result also seems reasonable—it makes sense that the two larger peaks adjacent to the smaller C5 component on either side of it could be used to compensate for changes in the position of C5 as long as it is not moved too far from its optimal position—this analysis suggests that there is some uncertainty in the position of this peak. The blue trace in Fig. 5 with the classic “V” shape for the large peak (C3 + C4) at 286.7 eV in Fig. 4(b) is a dramatic example of a component that is

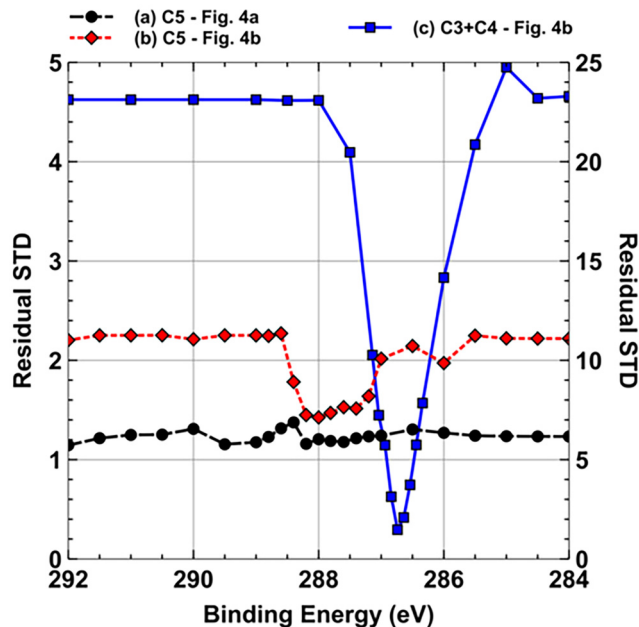


**FIG. 5.** Uniqueness plots for three different synthetic fit components in the peak fits shown in Figs. 4(a) and 4(b). In each case, the center energy of the peak was moved to a different position and then fixed at that position. The data were then refit, and the error of the fit was recorded (Residual STD). The (a) black circle (dashed line), (b) red diamond (dotted line), and (c) blue square (solid line) markers are the uniqueness plots for the synthetic peaks at 287.8 eV (C5) in Fig. 4(a), 287.8 eV (C5) in Fig. 4(b), and 286.7 eV (C3 + C4) in Fig. 4(b). See text for additional details.

clearly unique: the error in the fit rises sharply when the peak is forced to have a different position. This result again appears to be consistent with the fit in Fig. 4(b)—there is no adjacent component in the fit that can adequately compensate for changes in the synthetic peak at 286.7 eV. These results show that it can be necessary to generate more than one uniqueness plot for a fit. Note that the Monte Carlo analyses from Fig. 4 are consistent with the results in the uniqueness plots. Both analyses show that there is greater uncertainty in the small peaks at 287.8 eV in Figs. 4(c) and 4(d) than in the large peak at 286.7 eV in Fig. 4(d). Of course, uniqueness plots are not limited to peak position—they can be generated by systematically changing any parameter in a fit, e.g., FWHM.

Finally, we present here a different curve-fitting protocol, a protocol that instead of using synthetic line shapes makes use of the experimental spectra from the two pure compounds. In using only those two fit components, we assume that the mixed samples are simply physical mixtures of the two pure compounds, an assumption that may or may not be valid. The fitting results (shown in Fig. 6) suggest that this assumption is indeed valid, at least as a first approximation: all three fits are of an acceptable quality and information about relative surface fractions can easily be extracted. The integrated peak areas of the two components are a direct measure of the relative number of carbon atoms in each constituent and, by appropriate scaling, can be converted to relative

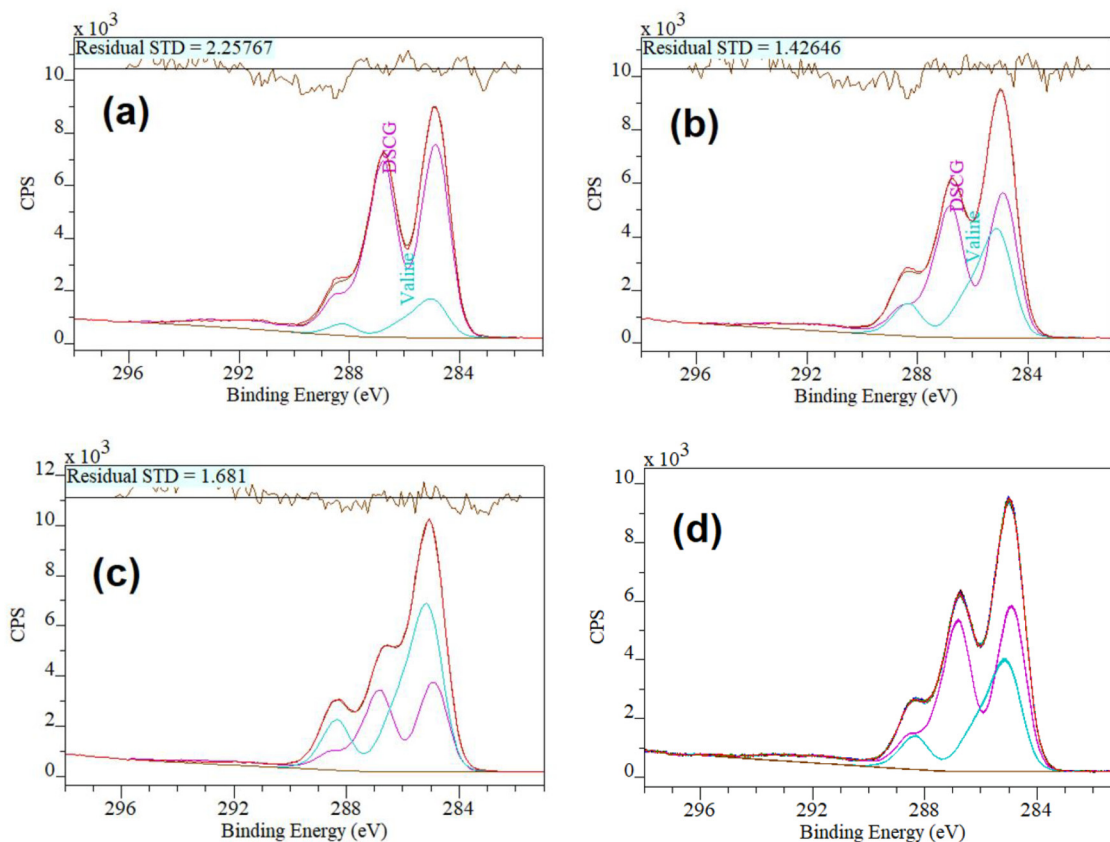


**FIG. 6.** (a)–(c) C 1s spectra of all three mixed samples fitted with the two reference spectra. (a) 67 mol. % DSCG-33 mol. % valine (b) 48 mol. % DSCG-52 mol. % valine (c) 26 mol. % DSCG-74 mol. % valine (d) Result of the Monte Carlo based test of the peak fit model (see text for details). CPS is photoelectron counts in counts/s.

molar fractions. Importantly, these values proved to be consistent with the corresponding values derived from the elemental compositions as mentioned above (data not shown). The overlay plot in Fig. 6(d) illustrates the results of our Monte Carlo analysis for the case of the same spectrum analyzed in Fig. 4. It is obvious that there is only minimal variation in peak parameters with the peak areas only varying by less than 1%.

### APPENDIX B: USING C 1s SPECTRA OF ADVENTITIOUS CARBON FOR CHARGE CORRECTION

Using the C 1s spectrum of adventitious carbon (AdC) as a reference for charge correction has remained a very popular method since it was first introduced by Siegbahn and co-workers more than 50 years ago. However, this method has significant limitations and is based on assumptions that are not always valid.<sup>1</sup> Within these limitations, it is still a very useful method for charge correction, and in the day-to-day work of an analytical laboratory, it is often the only practical method for charge correction available to the analyst. Indeed, it is often a simple and effective method for

charge correction if the only goals of an analysis are peak identification and fitting of those peaks.

As shown in Fig. 7, C 1s spectra of adsorbed AdC tend to have remarkably similar peak shapes irrespective of the substrate material: a reasonably narrow, intense peak at the lowest peak energy with minor peaks at higher energies. The lack of any  $\pi \rightarrow \pi^*$  shake up structure about 6–15 eV above the main peak (characteristic for aromatic groups) and the presence of oxygen (detected via survey spectra) leads to the following reasonable assumptions: the main peak is due to aliphatic hydrocarbon (C–C, C–H) and the minor peaks are due to a range of carbon-oxygen based functional groups, most commonly C–O based (+1.2–1.5 eV) and O–C=O based (+3.5–4.5 eV). The actual nature of the AdC layer is not really important as long as the assignment of the main peak is valid.

A simple peak fit of the AdC C 1s spectrum, taking into account the main hydrocarbon peak as well as the possible range of carbon-oxygen groups (C–O at ca. +1.5 eV, C=O at ca. +3 eV and O–C=O at ca. +4 eV), is generally sufficient to determine the measured position of the main peak [Figs. 7(c) and 7(d)]. Importantly, this position can be determined quite precisely because there is only weak interference from the minor peaks at

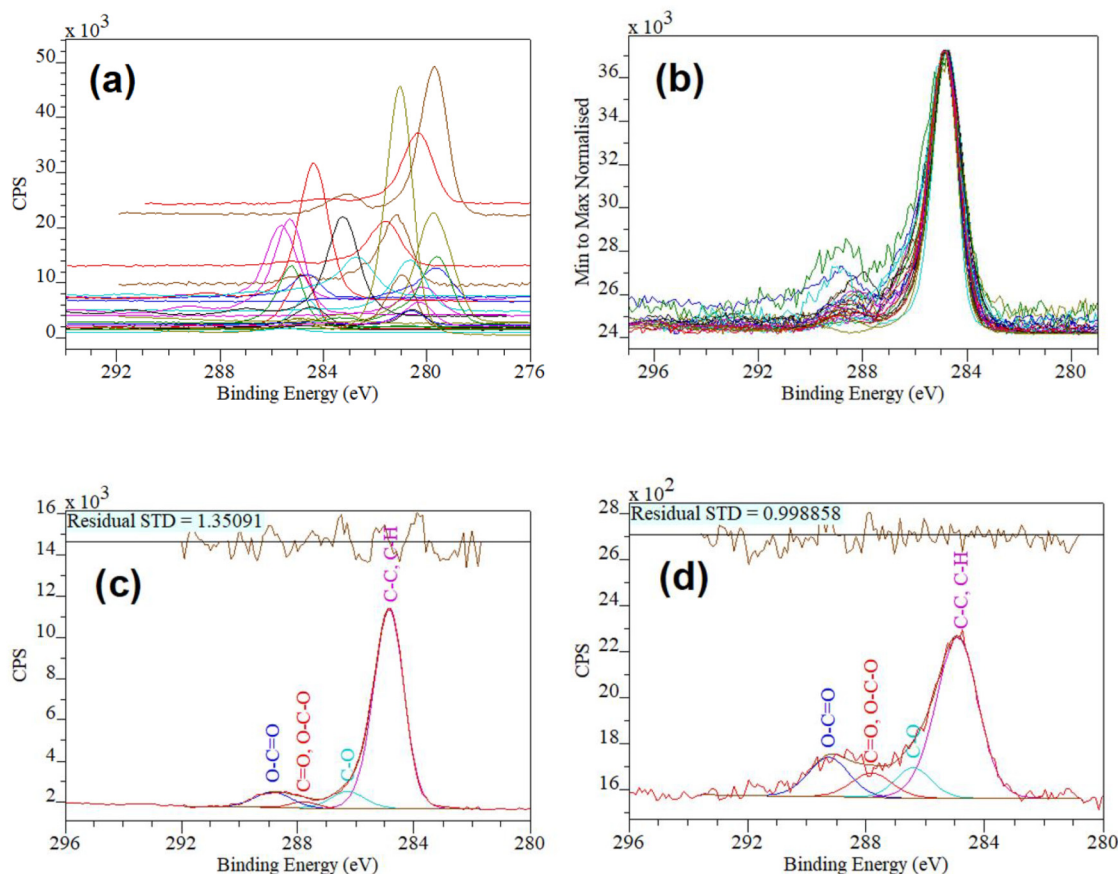


**FIG. 7.** Compilation of AdC C 1s spectra recorded on two instruments in one analytical laboratory over a 2-year period on a wide range of different materials (Au, Ag, Cu, Ni, Pb, Li, Ti/Ta alloy, AlTiVCr alloy, 316 Stainless Steel, Si wafer, Si nanoparticles, NiO, In<sub>2</sub>O<sub>3</sub>, ZrO<sub>2</sub>, CeO<sub>2</sub>, BiVO<sub>4</sub>, TiO<sub>2</sub>, ITO, Co Bi oxide, Nb oxynitride, V nitride, CoMoS, CoMo<sub>4</sub>, and AgBiS<sub>2</sub>). (a) Raw data acquired under a range of different conditions, with the sample being either grounded or isolated, and with the charge neutralizer either switched on or off. (b) The same data but where the peak intensity has been normalized (min. to max.), and the peak energy of the main peak has been set to 284.8 eV. (c) and (d) Two examples of AdC C 1s spectra (recorded on Cu and ZrO<sub>2</sub>) with simple four component fits to determine the peak energy of the aliphatic hydrocarbon peak (set here to 284.8 eV). CPS is photoelectron counts in counts/s.

higher binding energy. As described in ISO and ASTM guides, it is assumed that the C—C/C—H component of the measured C 1s spectrum of AdC would have a binding energy in the range of 284.6–285.0 eV and that the necessary correction can be determined from the measured peak and applied as a constant shift to all other spectra from the same analysis.<sup>18,19</sup> This charge correction is generally a good starting point for peak assignments, subject, of course, to the caveats described in the XPS guide on charge neutralization.<sup>1</sup>

### APPENDIX C: FITTING THE C 1s SPECTRUM OF GRAPHITIC AND MIXED GRAPHITIC/NONGRAPHITIC MATERIALS

#### Background

Our prior work showed that the peak fitting of graphitic materials is the largest contributor to errors in peak fitting C 1s spectra in

the published literature.<sup>2</sup> This observation is not surprising; materials such as graphene and graphene oxide (GO) have been the focus of intense research in recent years, and the C 1s spectral envelopes of these rather advanced materials are difficult to fit without careful consideration of their physical and chemical properties.

The aim of this appendix is to provide the reader with examples of how to fit the C 1s spectra of graphitic materials. Here, we apply the strategies described in this guide to data collected by the authors and published elsewhere.<sup>76–78</sup>

#### Analysis

Data were analyzed from five samples: freshly cleaved highly oriented pyrolytic graphite (HOPG; commercial sample), CVD graphene, graphene powder (commercial sample), graphene oxide (GO), and reduced GO (rGO).



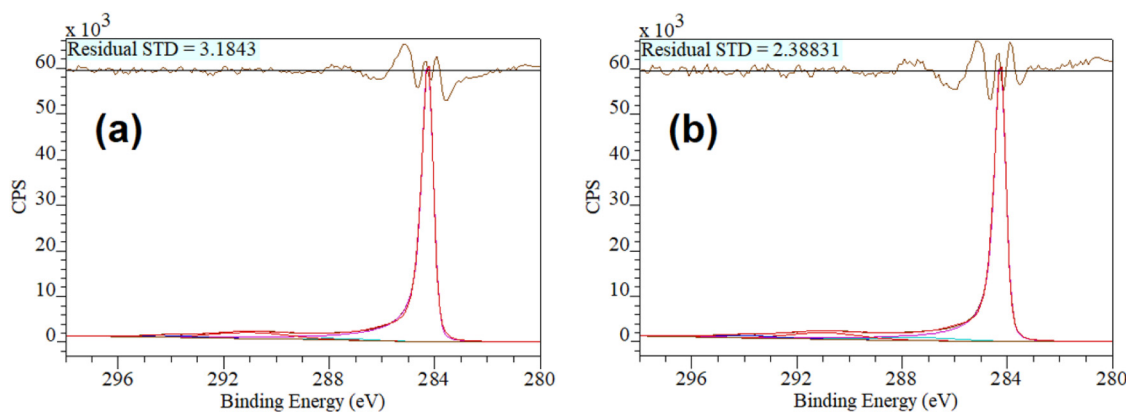


**FIG. 8.** Peak fitting of the high-resolution C 1s spectrum of HOPG. (a) Initial fit using Fairley's step-by-step fitting protocol (see text). (b) Final fit after further refinements (see text for details). CPS is photoelectron counts in counts/s.

When designing an XPS experiment, it is important to consider analyzing appropriate control samples to aid in data interpretation. In the context of graphitic materials with varying amounts of carbon-oxygen groups, HOPG was included to provide a pure graphitic carbon C 1s spectrum as a basis for defining the background type and component line shapes. The starting point for this analysis was a fitting protocol developed by Neil Fairley of CasaXPS (see the following YouTube video for a walkthrough: <https://www.youtube.com/watch?v=PhsQ60jHzkU>), which was applied to the HOPG data [Fig. 8(a)]. This fit was further refined by the authors [Fig. 8(b)]; we changed the background line shape from the U 2 Tougaard to the more flexible U 3 Tougaard background and made some minor changes to the component peak shapes to lower the residual STD value (Table III).

Even though it only has one type of carbon atom in its network, four components were needed to fit the C 1s spectrum of HOPG because of peak asymmetry in the main peak and a shake-up signal. Indeed, it was not possible to capture the asymmetry of the main peak with a single component (three were required). This fit of HOPG provided the line shapes and intensity ratios between the components that could be applied as constraints/fit parameters to the other fits of graphitic carbon considered here to account for the presence of graphitic/HOPG-like signal. No components associated

with aliphatic carbon-oxygen groups were included, as no oxygen was observed in the survey spectrum (data not shown).

The HOPG fit was propagated/applied to the spectra from the three graphitic carbon samples with carbon-oxygen species: CVD graphene (Fig. 9), graphene powder (Fig. 10), and rGO [Fig. 11(a)]. Additional components were then added to these fits to account for aliphatic carbon species, specifically C–C/C–H (284.7–284.9 eV), C–O and C–N (286.1–286.4 eV), C=O and O–C–O (287.8–288 eV), and O–C=O (288.8–289.3 eV). The limited ranges listed for these fit components were used to ensure that their positions (eV) and FWHM (eV) values did not move beyond acceptable limits. Nevertheless, while the HOPG reference spectrum provided a good starting point for the graphitic signal in these fits, small changes to this peak shape were required to account for chemical and physical differences between the different graphitic materials and to reduce the figure of merit.

An internal check was performed to confirm that the fits were reasonable in relation to the proposed number of carbon-oxygen species; this process is necessary to avoid unrealistic fits. For example, it is not logical to have very large components for high BE contributions such as O–C=O if there is very little (or no) oxygen detected in the survey spectrum. Using the elemental quantification derived from survey spectra and the results of the high-resolution C

**TABLE III.** Curve fitting details for HOPG presented in Fig. 8. No charge correction was applied to the data.

Fit protocol	Background	Component	Lineshape	BE (eV)	FWHM (eV)	Intensity ratio
Fairley	U 2 Tougaard	C1	LF(0.6,1.14,455,200,3)	284.2	0.49	—
		C2	LF(1,1,255,360,6)	287.7	2.6	C3*0.23
		C3	"	291.0	3.4	1
		C4	"	294.2	2.2	C3*0.2
Final fit	U 3 Tougaard	C1	LF(0.65,1.17,550,180,2)	284.2	0.49	—
		C2	LF(1,1,255,300,6)	287.7	2.6	C3*0.55
		C3	LF(1,1,255,360,6)	291.0	3.4	1
		C4	"	294.2	2.2	C3 * 0.37

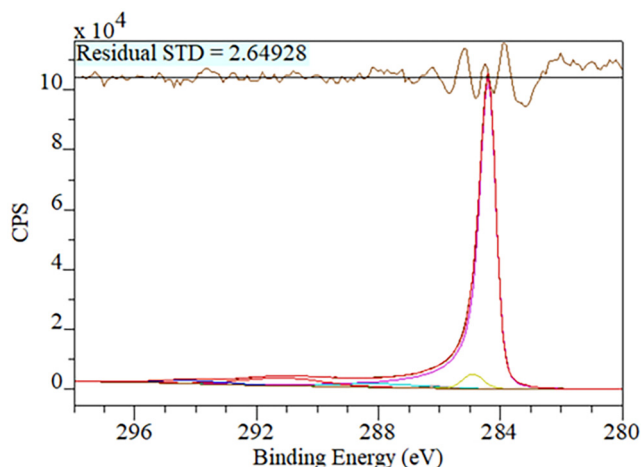


**FIG. 9.** High resolution C 1s spectrum of CVD graphene fitted using a standard protocol employing only synthetic components. CPS is photoelectron counts in counts/s.

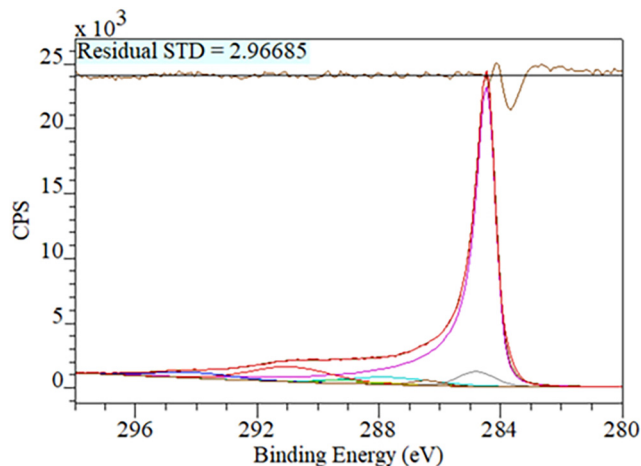


**FIG. 10.** High resolution C 1s spectrum of graphene powder fitted using a standard protocol employing only synthetic components. CPS is photoelectron counts in counts/s.

1s fitting (relative fraction of C components), the atomic% for each carbon component was calculated (data not shown). These values were used to estimate the atomic% of O associated with each carbon component using O/C multipliers based on assumptions regarding the relative fraction of carbon-oxygen species for each assignment (see Table IV for multipliers and assumptions). These values were then compared with the total O concentration derived from the survey spectra, and the relative difference was calculated (Table V). A detailed account for this type of analysis has been published previously.<sup>9</sup>

Previously, we stated that a difference of up to 10% between experimental and theoretical composition values would be considered reasonable;<sup>9</sup> in this example, a larger error would be expected

because the exact theoretical composition of these samples is not known and an educated guess for the O/C multipliers was made. Some of the samples also had small amounts of impurities that were also associated with O, such as SO<sub>x</sub> for the GO and rGO samples, and as such it would be unreasonable for the O concentration defined by the C 1s fit to equal that determined from the elemental quantification. In addition, as the total O concentration decreases, the relative error will become larger. Hence, a difference of 10%–15% is considered reasonable, i.e., the difference between the oxygen concentration derived from the survey spectra and the amount of O determined from the C 1s fits (Table V) is considered reasonable for CVD graphene, graphene powder, and rGO (standard fit). When making such judgement calls, it is important

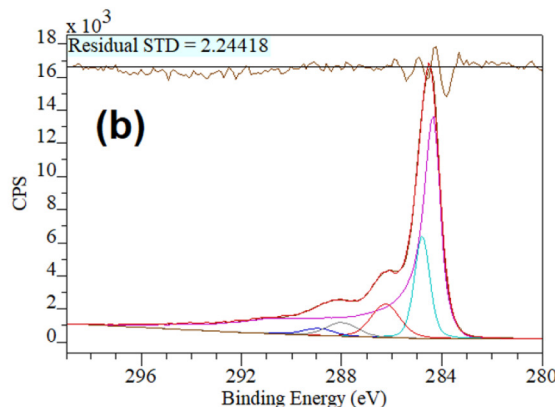
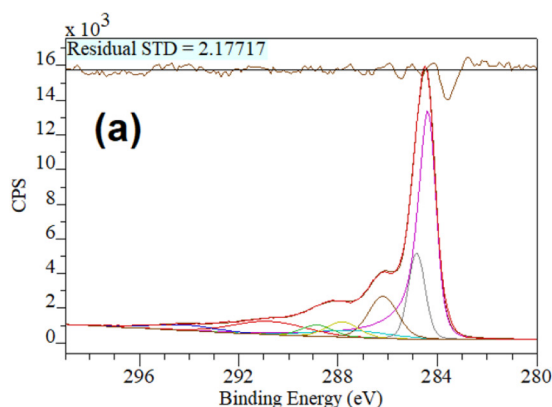


**FIG. 11.** High resolution C 1s spectrum of rGO, (a) fitted using a standard protocol employing only synthetic components and (b) fitted using a combination of synthetic components and a model spectrum component derived from experimental data. CPS is photoelectron counts in counts/s.

**TABLE IV.** O/C multipliers and the associated assumptions used for each component to estimate the atomic concentration of oxygen associated with each carbon component.

C 1s component	Assigned O/C value	Assumptions
C—O in CVD graphene	0.75	Equal ratio of epoxide (O/C = 0.5) and hydroxyl (O/C = 1)
C—O in GO	0.5	Bulk of C—O in GO is expected to be epoxide
C=O, O—C—O	1.5	Equal ratio of C=O (O/C = 1) and O—C—O (O/C = 2) groups
O—C=O	2	Very few to no ester groups

to consider that while the fits are considered reasonable based on this criterion, they may not be an accurate representation of the types and distribution of carbon-oxygen based functional groups; this is just one of many tests one should perform to ensure a robust fit. Another test would be to check the high-resolution O 1s spectra to see whether the types and relative fraction of O groups defined previously are rational.

To explore the best approach for fitting rGO, an alternative fit protocol was applied using the graphene powder spectrum as a model spectrum for the graphitic contribution [Fig. 11(b)]. The fit visually appears similar to the “standard” protocol employing only synthetic components, and it is easier to perform and interpret, particularly in the region above 288 eV as there is no longer overlapping of individual components. While the graphene powder spectrum appears to fit the high BE portion of the spectrum well, it is not necessarily an appropriate model spectrum for the whole region. Unlike the pharmaceutical example in Appendix A, rGO is not derived from graphene powder, but rather GO, meaning there is no model spectrum that is directly applicable in this case. The question then arises as to which of the two fits is the better representation and whether it is reasonable to use a model spectrum as a fit component, which will give results that will be easier to interpret. Undertaking the same test detailed above to check the O concentration defined by a C 1s fit, it is clear from Table V that the O concentration determined by rGO (model fit) is significantly different from that of the standard fit and the elemental quantification. With 0.6 at. % S (assuming SO<sub>3</sub>, O = 1.8 at. %) and 0.5 at. % Si (assuming Si—O, O = 0.5 at. %), we have approximately 2.3 at. % of O that is not associated with carbon. If we remove this oxygen out of the equation for rGO, the difference between the two O concentrations

**TABLE V.** Comparison of O concentration based on carbon-oxygen groups obtained via C 1s fits with oxygen concentration from elemental quantification (survey data).

Sample	Difference (%)
CVD graphene	-13.1
Graphene powder	9.7
rGO (standard fit)	-2.1
rGO (model fit)	17.8
GO	-3.4
Removing contribution from total O associated with elements other than C for rGO sample	
rGO (standard fit)	-15.4
rGO (model fit)	4.6

now becomes ~-15% for the standard fit and ~5% for the model fit. Thus, once we remove known contributions to O that are associated with elements other than carbon, the model spectrum fit is a better approximation in terms of representing the sample elemental quantification. The example presented above highlights the importance of considering the overall chemistry of the sample when devising the fit protocol for high resolution C 1s spectra.

GO is reported extensively in the literature where one can find a variety of fits to its C 1s spectra with significant variation in the quality of these fits. A common error here is overfitting, for example, adding separate components for graphitic and nongraphitic “neutral” carbon, and epoxide and hydroxyl groups. Considering the questions listed in Appendix A would be helpful in identifying any potential problems with a specific peak fit model, such as significant peak overlap, or the lack of a clear spectral feature that would justify the addition of an extra fit component. Unfortunately, examples exist in the literature where the contribution from hydroxyl groups conveniently increases or decreases in line with the story the authors wish to tell, but there is no obvious change in the spectral envelope to justify these changes, and no internal consistency check is performed regarding overall oxygen concentrations. While the authors may (or may not, considering this is rarely reported!) have obtained a low residual STD value for their fit, it is very easy to obtain a series of

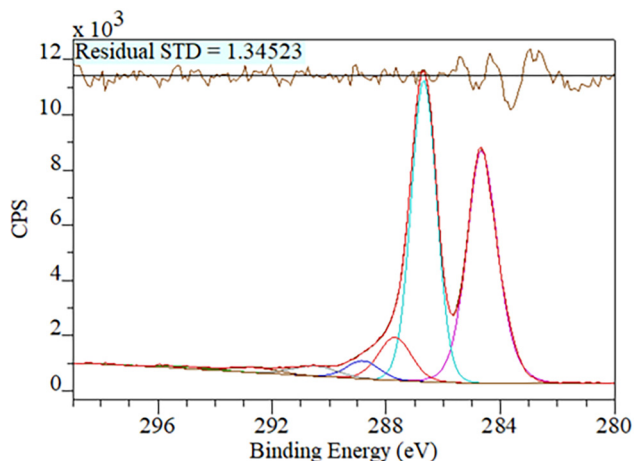


**FIG. 12.** C 1s spectrum of GO, including the recommended curve-fit (see text for details). CPS is photoelectron counts in counts/s.

nonunique fits when fitting is approached in this manner, as will be demonstrated below.

A recommended fit for GO is provided in Fig. 12, with four components at 284.7 eV (C=C, C-C, C-H), 286.7 eV (C-O groups), 287.7 eV (C=O, O-C-O), and 288.8 eV (O-C=O), plus two additional components at 290.5 and 292.5 eV to account for aromatic shake-up features. The spectrum was fitted using a “U 3 Tougaard” background and Voigt line shapes, a slightly asymmetric component for reduced carbon (C=C, C-C, C-H), and a symmetric line shape for the remaining components. A series of fits using separate components for epoxide (light blue) and hydroxyl (yellow) is presented in Fig. 13. The hydroxyl component was fixed to a narrow BE region based on the mean position value given by Beamson and Briggs.<sup>10</sup> The peak area for the hydroxyl component in the first example was set to zero before fitting, resulting in the final fit in Fig. 13(a). For the subsequent two examples [Figs. 13(b) and 13(c)], the intensity for the hydroxyl component was manually increased before fitting, resulting in the two final fits presented. It is clear that none of these fits

are unique, with the minimization algorithm converging toward a different local minimum in each case. The other error analysis methods described in the main text could also be used here to confirm the obvious problem in determining the concentration of hydroxyls reliably; however, it can be observed easily in this case by a manual manipulation of the corresponding component before fitting, using an iterative approach. Finally, we note that the changing intensity ratio of hydroxyl to epoxide components observed in Figs. 13(a)–13(c) also affects the intensity of the other two carbon-oxygen components. The net effect represented by these carbon-oxygen based groups is an increase in the overall oxygen concentration with increasing intensity of the hydroxyl component. Considering that the original fit already overestimated the concentration of oxygen associated with carbon (Table V—negative difference value), this is additional confirmation that these fits cannot be justified. This example clearly demonstrates the importance of performing a combination of internal checks to ensure the chosen peak fit model generates reliable results that can be interpreted with confidence.

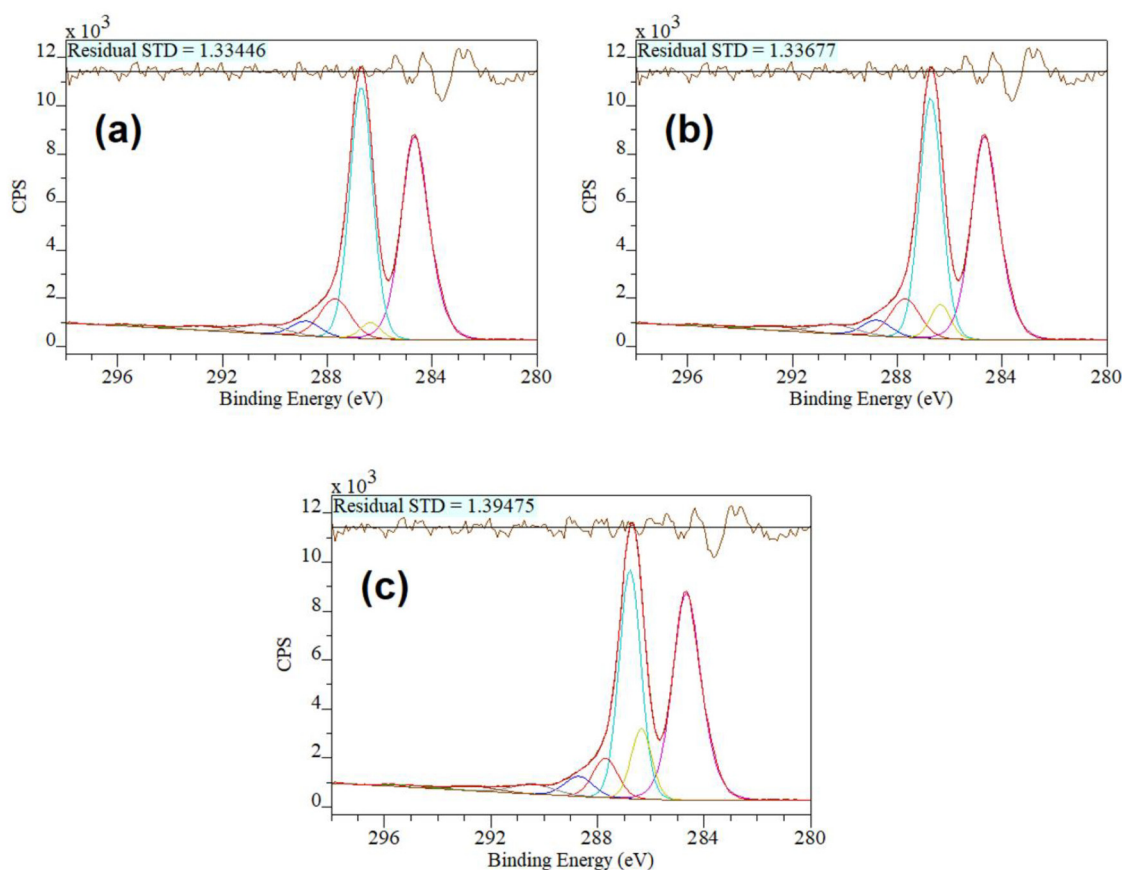


**FIG. 13.** High resolution C 1s spectrum of GO from Fig. 12 demonstrating instances of overfitting, with (a), (b), and (c) presenting three examples of fitted spectra with increasing OH- contribution; the component intensity was manually adjusted prior to using the minimization algorithm to give a new fit result. CPS is photoelectron counts in counts/s.

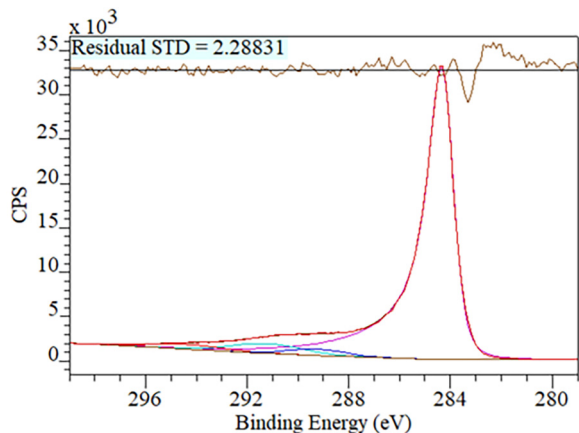


**FIG. 14.** CF reference sample fitted using the standard method (only synthetic components) (see text for details). CPS is photoelectron counts in counts/s.

## Part 2: Functionalization of carbon fibers with acrylic acid

### Background

In Part 1, we demonstrated a generalized approach to fitting C 1s spectra from graphitic carbon materials. Here we will apply both a standard fit using synthetic line shapes and a fit using model spectra to a series of functionalized graphitic carbon samples. CFs are widely used and researched because of their importance in CF-reinforced polymer composite materials. Their superior mechanical properties depend to a large extent on good adhesion between the fiber and the polymer matrix. Modification of the fiber surface is one of the most common methods investigated to enhance and optimize adhesion.

### Analysis

A series of CF samples that had been treated in solutions of increasing molar concentrations of acrylic acid with the aim of

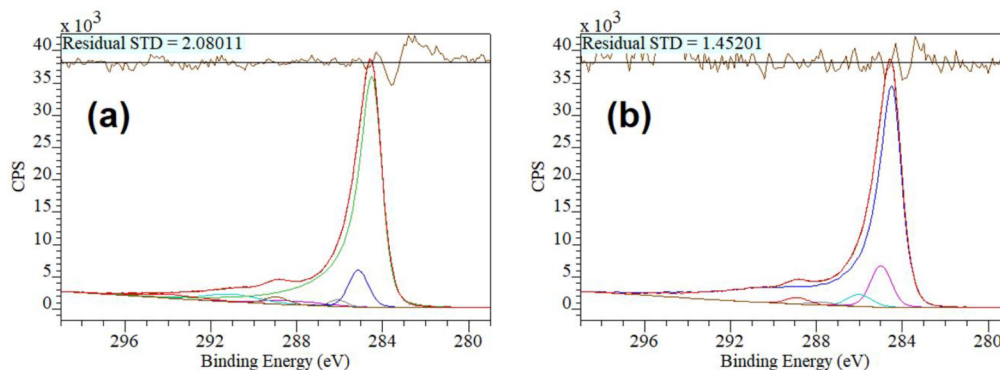


**FIG. 15.** High-resolution C 1s spectrum of (CF + 0.2 M AA) fitted using (a) standard fit (only synthetic components), and (b) model fit (model spectrum and synthetic components). CPS is photoelectron counts in counts/s.

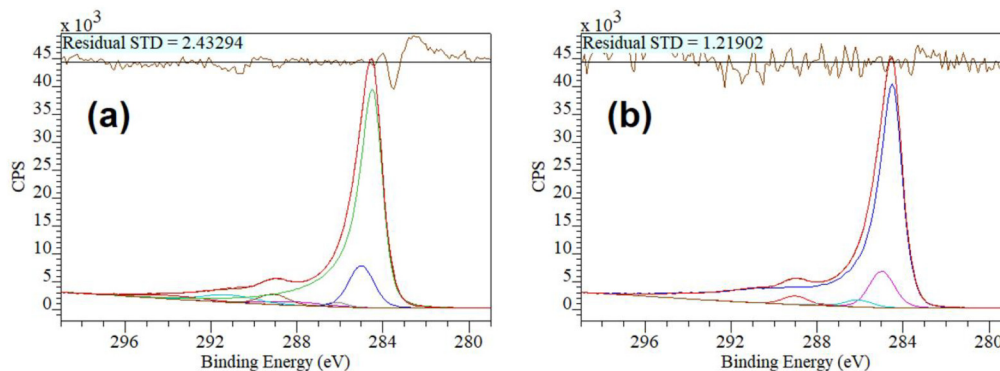


**FIG. 16.** High-resolution C 1s spectrum of (CF + 1.0 M AA) fitted using (a) standard fit (only synthetic components), and (b) model fit (model spectrum as well as synthetic components). CPS is photoelectron counts in counts/s.

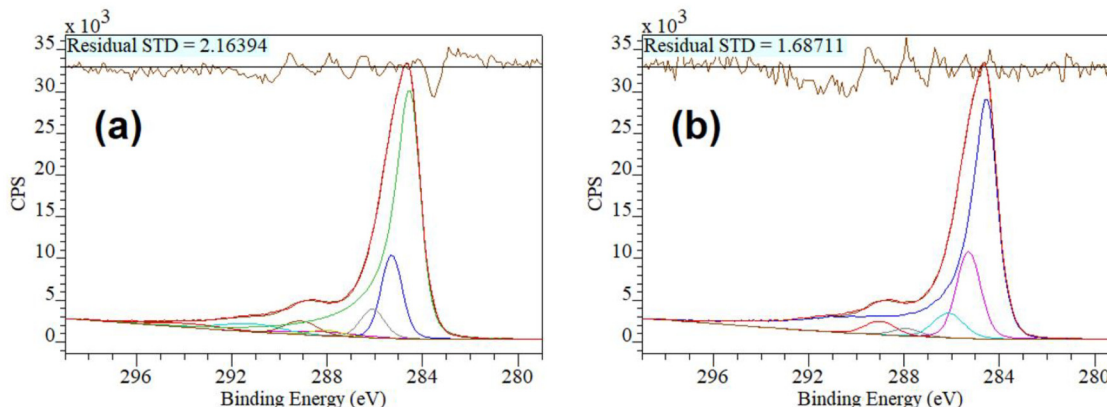


**FIG. 17.** High-resolution C 1s spectrum of CF + 1.5 M AA fitted using (a) standard fit (only synthetic components), and (b) model fit (model spectrum as well as synthetic components). CPS is photoelectron counts in counts/s.

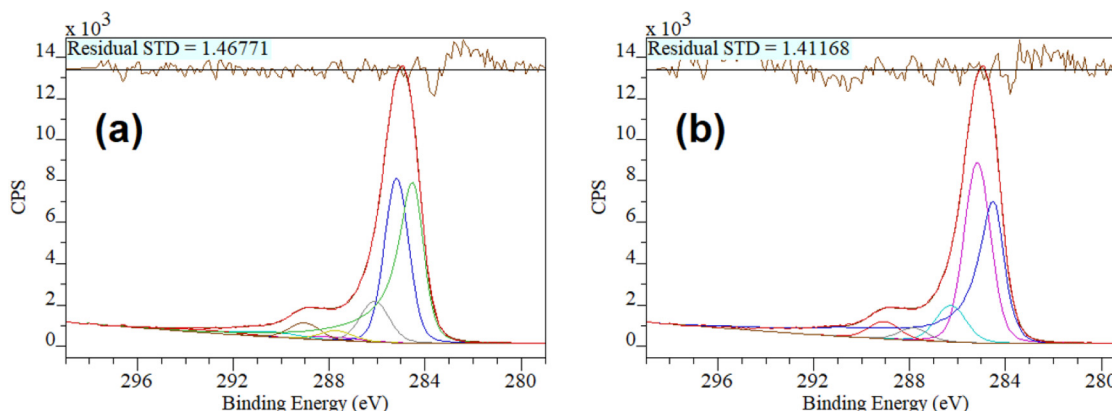


**FIG. 18.** High-resolution C 1s spectrum of CF + 2.0 M AA fitted using (a) standard fit (only synthetic components) and (b) model fit (model spectrum as well as synthetic components). CPS is photoelectron counts in counts/s.

**TABLE VI.** Comparison of the O–C=O component concentration (at. %) for a series of CF samples with increasing acrylic acid concentrations derived using two different fitting protocols. Values shown are the mean ( $\pm$  standard deviation) of several measurements per sample. Note that this uncertainty does not take into account any error introduced by the fitting process.

Sample	Fit approach	O–C=O concentration (at. %)	
		Mean	(SD)
CF + 0.2M	Standard	1.4	(0.2)
	Model	1.3	(0.2)
CF + 1.0M	Standard	2.4	(0.2)
	Model	1.9	(0.3)
CF + 1.5M	Standard	2.9	(0.1)
	Model	2.7	(0.1)
CF + 2.0M	Standard	3.7	(0.7)
	Model	3.8	(0.5)

grafting an acrylic acid polymer coating to the surface were analyzed, in addition to an as-received CF reference sample. The aim of the analysis was to confirm and quantify functionalization of the CF by focusing on the C 1s signal of the acrylic acid groups.

The CF reference was fitted with a series of four components (Fig. 14) following the same principles as for the HOPG fit described above, which provided line shapes and intensity ratios for the standard fit protocol. Unlike the HOPG reference, the CF sample has some impurities including O and N that are likely associated with carbon. It is unclear whether these impurities are fixed to the surface or if their concentration will be impacted during the functionalization step, which will be a source of uncertainty in the analysis.

A series of C 1s spectra from CF samples that had been modified in 0.2, 1.0, 1.5, and 2 M solutions of acrylic acid, fitted using both approaches (standard fit using synthetic line shapes and a fit using the CF reference spectrum as a model

component), are presented in Figs. 15–18. Both fit protocols use four additional components for aliphatic carbon associated with the polymerized acrylic acid on the surface of the CF, similar to the fit in Part 1. As with the fitting comparison detailed above for rGO, fitting with model spectra provides a fit of a mixed graphitic/nongraphitic sample that is easier to perform and interpret: instead of having to use multiple parameter constraints for multiple component peaks to maintain the asymmetric CF peak shape, only one single model component is required. Setup and application of the fit are, therefore, simplified significantly.

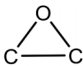
A comparison of the atomic concentrations of the O–C=O (acid) component for the CF series is provided in Table VI. Generally, there was minimal difference between the results of the two fitting

protocols within experimental uncertainty. The objective of the analysis was achieved: C 1s analysis enabled identification and quantification of acrylic acid groups on the modified CF surfaces, and the observed trend correlated with an increase in the molar concentration of acrylic acid in solution. Considering the advantages described above, the peak fit model based on the reference spectrum of unmodified CF would clearly be the preferred choice in this instance.

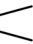

#### APPENDIX D: PRIMARY AND SECONDARY C 1s CHEMICAL SHIFTS

Tables VII–X are based on the polymer XPS database published by Beamson and Briggs in 1992, a database that remains one

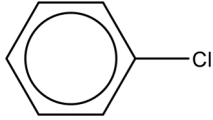
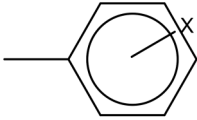
**TABLE VII.** Primary chemical shifts (oxygen functions).

Functional group	Mean chemical shift (eV)	Functional group	Mean chemical shift (eV)
$\text{C}-\text{O}-\text{C}$	1.45	$\text{C}-\text{O}-\overset{*}{\text{C}}$ $\parallel$ $\text{O}$	3.99
$\text{C}-\text{OH}$	1.55	$\text{HO}-\text{C}$ $\parallel$ $\text{O}$	4.26
$\text{C}^*-\text{O}-\text{C}$ $\parallel$ $\text{O}$	1.64	$\text{O}-\text{C}-\text{O}$ $\parallel$ $\text{O}$	4.32
	2.02	$\text{---C}-\text{O}-\text{C---}$ $\parallel \quad \parallel$ $\text{O} \quad \text{O}$	4.41
$\text{C}=\text{O}$	2.90	$\text{---O}-\text{C}-\text{O---}$ $\parallel$ $\text{O}$	5.40
$\text{O}-\text{C}-\text{O}$	2.93		

**TABLE VIII.** Primary chemical shifts (nitrogen functions).

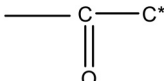
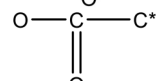
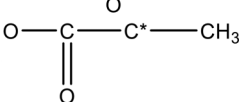
Functional group	Mean chemical shift (eV)	Functional group	Mean chemical shift (eV)
$\text{C}-\text{NO}_2$	0.76	$\text{N}-\text{C}-\text{O}$	2.78
$\text{C}-\text{N}$ 	0.94	$\text{N}-\text{C}=\text{O}$	3.11
$\text{C}-\text{N}^+$ 	1.11	$\text{C}-\text{N}-\text{C}$ $\parallel \quad \parallel$ $\text{O} \quad \text{O}$	3.55
$^*\text{C}-\text{C}\equiv\text{N}$	1.41	$\text{N}-\text{C}-\text{N}$ $\parallel$ $\text{O}$	3.84
$\text{---C}\equiv\text{N}$	1.74	$\text{N}-\text{C}-\text{O}$ $\parallel$ $\text{O}$	4.60
$\text{C}-\text{ONO}_2$	2.62		

**TABLE IX.** Primary chemical shifts (miscellaneous and halogen functions).

Functional group	Mean chemical shift (eV)	Functional group	Mean chemical shift (eV)
C=C	-0.27		1.02 <sup>a</sup>
	-0.34	C—Cl	2.02
C—Si	-0.67	—CCl <sub>2</sub>	3.56
C—S	0.37	C—F	2.91
C—SO <sub>2</sub>	0.38	—CF <sub>2</sub>	5.90
C—SO <sub>3</sub> <sup>-</sup>	0.16	—CF <sub>3</sub>	7.69
C—Br	0.74		

<sup>a</sup>Only C atom directly bonded to Cl experiences the chemical shift.

**TABLE X.** Secondary C 1s chemical shifts.

Functional group	Mean chemical shift (eV)	Functional group	Mean chemical shift (eV)
O—C—C*	~0.2		~0.4
F—C—C*	~0.4		~0.4
Cl—C—C*	~0.5		~0.7

of the most important resources for scientists interested in the XPS analysis of polymer surfaces.<sup>10</sup> The tables compile values of chemical shifts, both primary and secondary, relative to saturated hydrocarbon (C 1s = 285.00 eV) for a wide range of functional groups. Reported here are the mean values for all examples of the same functional group; for more details, including details about the experimental and analytical protocol, the reader is referred to the original database.<sup>10</sup>

## DATA AVAILABILITY

The data that support the findings of this study are available from the corresponding author upon reasonable request.

## REFERENCES

- <sup>1</sup>D. R. Baer *et al.*, *J. Vac. Sci. Technol. A* **38**, 031204 (2020).
- <sup>2</sup>G. H. Major *et al.*, *J. Vac. Sci. Technol. A* **38**, 061204 (2020).
- <sup>3</sup>D. R. Baer and I. S. Gilmore, *J. Vac. Sci. Technol. A* **36**, 068502 (2018).
- <sup>4</sup>M. Munafò, *Nature* **576**, 183 (2019).
- <sup>5</sup>D. Bishop, *Nature* **568**, 435 (2019).
- <sup>6</sup>M. R. Linford *et al.*, *Microsc. Microanal.* **26**, 1 (2020).

- <sup>7</sup>D. R. Baer *et al.*, *J. Vac. Sci. Technol. A* **37**, 031401 (2019).

<sup>8</sup>Special Topic Collection: Reproducibility Challenges and Solutions, *J. Vac. Sci. Technol. A* (2020), see <https://avs.scitation.org/topic/special-collections/reprod2020?SeriesKey=jva>

- <sup>9</sup>F. A. Stevie and C. L. Donley, *J. Vac. Sci. Technol. A* **38**, 063204 (2020).

<sup>10</sup>G. Beamson and D. Briggs, *High Resolution XPS of Organic Polymers the Scientia ESCA300 Database* (Wiley, Chichester, 1992).

- <sup>11</sup>C. D. Easton, C. Kinnear, S. L. McArthur, and T. R. Gengenbach, *J. Vac. Sci. Technol. A* **38**, 023207 (2020).

<sup>12</sup>F. A. Stevie, R. Garcia, J. Shallenberger, J. G. Newman, and C. L. Donley, *J. Vac. Sci. Technol. A* **38**, 063202 (2020).

- <sup>13</sup>D. I. Patel, S. Noack, C. D. Vacogne, H. Schlaad, S. Bahr, P. Dietrich, M. Meyer, A. Thißen, and M. R. Linford, *Surf. Sci. Spectra* **26**, 024004 (2019).

<sup>14</sup>A. Naumkin, A. Kraut-Vass, S. Gaarenstroom, and C. Powell, NIST X-ray Photoelectron Spectroscopy Database, NIST Standard Reference Database Number 20 (National Institute of Standards and Technology, Gaithersburg, MD, 2000).

- <sup>15</sup>D. R. Baer, C. F. Windisch, M. H. Engelhard, and K. R. Zavadi, *J. Surf. Anal.* **9**, 396 (2002).

<sup>16</sup>D. I. Patel *et al.*, *Surf. Sci. Spectra* **26**, 016801 (2019).

- <sup>17</sup>T. G. Avval, S. Chatterjee, S. Bahr, P. Dietrich, M. Meyer, A. Thißen, and M. R. Linford, *Surf. Sci. Spectra* **26**, 014022 (2019).

<sup>18</sup>V. Jain *et al.*, *Surf. Sci. Spectra* **26**, 024010 (2019).

- <sup>19</sup>D. S. Jensen *et al.*, *Surf. Interface Anal.* **45**, 1273 (2013).



- <sup>20</sup>A. M. Spool, *The Practice of TOF-SIMS: Time of Flight Secondary Ion Mass Spectrometry* (Momentum Press, New York, 2016).
- <sup>21</sup>S. Fearn, *An Introduction to Time-of-Flight Secondary Ion Mass Spectrometry (ToF-SIMS) and Its Application to Materials Science* (Morgan & Claypool, San Rafael, CA, 2015).
- <sup>22</sup>J. Wolstenholme, *Auger Electron Spectroscopy: Practical Application to Materials Analysis and Characterization of Surfaces, Interfaces, and Thin Films* (Momentum Press, New York, 2015).
- <sup>23</sup>G. G. Hoffmann, *Raman Spectroscopy, Volume I: Principles and Applications in Chemistry, Physics, Materials Science, and Biology* (Momentum Press, New York, 2019).
- <sup>24</sup>H. G. Tompkins and J. N. Hilfiker, *Spectroscopic Ellipsometry: Practical Application to Thin Film Characterization* (Momentum, New York, 2015).
- <sup>25</sup>H. Fujiwara, *Spectroscopic Ellipsometry: Principles and Applications* (John Wiley & Sons, Hoboken, 2007).
- <sup>26</sup>ASTM E1523-15, *Standard Guide to Charge Control and Charge Referencing Techniques in X-Ray Photoelectron Spectroscopy* (ASTM International, West Conshohocken, 2015).
- <sup>27</sup>ISO 19318:2004, Surface chemical analysis—X-ray photoelectron spectroscopy—Reporting of methods used for charge control and charge correction, International Organization for Standardization, Geneva, 2004.
- <sup>28</sup>G. Greczynski and L. Hultman, *Prog. Mater. Sci.* **107**, 100591 (2020).
- <sup>29</sup>V. Jain, M. C. Biesinger, and M. R. Linford, *Appl. Surf. Sci.* **447**, 548 (2018).
- <sup>30</sup>T. Susi, T. Pichler, and P. Ayala, *Beilstein J. Nanotechnol.* **6**, 177 (2015).
- <sup>31</sup>R. Blume, D. Rosenthal, J. P. Tessonier, H. Li, A. Knop-Gericke, and R. Schlögl, *ChemCatChem* **7**, 2871 (2015).
- <sup>32</sup>D. S. Jensen, S. S. Kanyal, N. Madaan, M. A. Vail, A. E. Dadson, M. H. Engelhard, and M. R. Linford, *Surf. Sci. Spectra* **20**, 62 (2013).
- <sup>33</sup>G. H. Major, D. Shah, V. Fernandez, N. Fairley, and M. R. Linford, *Vac. Tech. Coat.* **21**, 43–46 (2020).
- <sup>34</sup>G. H. Major, D. Shah, V. Fernandez, N. Fairley, and M. R. Linford, *Vac. Tech. Coat.* **21**, 35–39 (2020).
- <sup>35</sup>S. Doniach and M. Sunjic, *J. Phys. C Solid State Phys.* **3**, 285 (1970).
- <sup>36</sup>H. Ganegoda, D. S. Jensen, D. Olive, L. Cheng, C. U. Segre, M. R. Linford, and J. Terry, *J. Appl. Phys.* **111**, 053705 (2012).
- <sup>37</sup>G. H. Major, N. Fairley, P. M. Sherwood, M. R. Linford, J. Terry, V. Fernandez, and K. Artyushkova, *J. Vac. Sci. Technol. A* **38**, 061203 (2020).
- <sup>38</sup>B. Singh, R. Hesse, and M. R. Linford, *Vac. Tech. Coat.* **12**, 25–31 (2015).
- <sup>39</sup>B. Singh, A. Herrera-Gomez, J. Terry, and M. R. Linford, *Vac. Tech. Coat.* **17**, 24–27 (2016).
- <sup>40</sup>P. M. A. Sherwood, *Surf. Interface Anal.* **51**, 589 (2019).
- <sup>41</sup>P. M. A. Sherwood, *J. Vac. Sci. Technol. A* **14**, 1424 (1996).
- <sup>42</sup>J. Matthew, D. Briggs, and J. T. Grant, *Surface Analysis by Auger and X-Ray Photoelectron Spectroscopy* (IMP Publications, Chichester, 2004).
- <sup>43</sup>B. Singh, A. Diwan, V. Jain, A. Herrera-Gomez, J. Terry, and M. R. Linford, *Appl. Surf. Sci.* **387**, 155 (2016).
- <sup>44</sup>E. S. Mark Greiner, John Walton, David Morgan, Vincent Fernandez, Jonas Baltrusaitis, and Neal Fairley, “A guide to fitting XPS data with peaks,” *J. Vac. Sci. Technol. A* (unpublished).
- <sup>45</sup>D. R. Baer and A. G. Shard, *J. Vac. Sci. Technol. A* **38**, 031203 (2020).
- <sup>46</sup>R. N. Bracewell, *The Fourier Transform and Its Applications*, 3rd ed. (McGraw-Hill, New York, 1999).
- <sup>47</sup>J. E. Castle, *Surf. Interface Anal.* **33**, 196 (2002).
- <sup>48</sup>A. S. Lea, K. R. Swanson, J. N. Haack, J. E. Castle, S. Tougaard, and D. R. Baer, *Surf. Interface Anal.* **42**, 1061 (2010).
- <sup>49</sup>M. Correll and J. Heer, paper presented at the Proceedings of the 2017 CHI Conference on Human Factors in Computing Systems, Denver, 2 May 2017.
- <sup>50</sup>D. I. Patel, A. Matic, H. Schlaad, S. Bahr, P. Dietrich, M. Meyer, and A. Thißen, *Surf. Sci. Spectra* **27**, 014005 (2020).
- <sup>51</sup>T. Roychowdhury, S. Bahr, P. Dietrich, M. Meyer, A. Thißen, and M. R. Linford, *Surf. Sci. Spectra* **26**, 014018 (2019).
- <sup>52</sup>D. Shah, D. I. Patel, T. Roychowdhury, G. B. Rayner, N. O’Toole, D. R. Baer, and M. R. Linford, *J. Vac. Sci. Technol. B* **36**, 062902 (2018).
- <sup>53</sup>G. H. Major, T. G. Avval, N. Fairley, and M. R. Linford, *Vac. Tech. Coat.* **21**, 37–40 (2020).
- <sup>54</sup>M. H. Engelhard, D. R. Baer, A. Herrera-Gomez, and P. M. Sherwood, *J. Vac. Sci. Technol. A* **38**, 063203 (2020).
- <sup>55</sup>S. Tougaard, *J. Vac. Sci. Technol. A* **39**, 011201 (2021).
- <sup>56</sup>G. H. Major, T. G. Avval, D. I. Patel, D. Shah, T. Roychowdhury, A. J. Barlow, P. J. Pigram, M. Greiner, V. Fernandez, A. Herrera-Gomez, N. Fairley, and M. R. Linford, “Practical guides for x-ray photoelectron spectroscopy (XPS): Synthetic line shapes for fitting asymmetric signals,” *J. Vac. Sci. Technol. A* (submitted).
- <sup>57</sup>M. C. Biesinger, L. W. Lau, A. R. Gerson, and R. S. C. Smart, *Appl. Surf. Sci.* **257**, 887 (2010).
- <sup>58</sup>D. A. Beattie, A. Arcifa, I. Delcheva, B. A. Le Cerf, S. V. MacWilliams, A. Rossi, and M. Krasowska, *Colloids Surf. A* **544**, 78 (2018).
- <sup>59</sup>Q. Liu, Y. Han, J. Cai, E. J. Crumlin, Y. Li, and Z. Liu, *Catal. Lett.* **148**, 1686 (2018).
- <sup>60</sup>American Vacuum Society, see <https://avs.scitation.org/journal/sss> for “Surface Science Spectra.”
- <sup>61</sup>P. R. Davies and D. J. Morgan, *J. Vac. Sci. Technol. A* **38**, 033204 (2020).
- <sup>62</sup>A. G. Shard, *J. Vac. Sci. Technol. A* **38**, 041201 (2020).
- <sup>63</sup>C. R. Brundle and B. V. Crist, *J. Vac. Sci. Technol. A* **38**, 041001 (2020).
- <sup>64</sup>J. Wolstenholme, *J. Vac. Sci. Technol. A* **38**, 043206 (2020).
- <sup>65</sup>T. G. Avval, G. T. Hodges, J. Wheeler, D. H. Ess, S. Bahr, P. Dietrich, M. Meyer, A. Thißen, and M. R. Linford, *Surf. Sci. Spectra* **27**, 014006 (2020).
- <sup>66</sup>T. Roychowdhury, S. Bahr, P. Dietrich, M. Meyer, A. Thißen, and M. R. Linford, *Surf. Sci. Spectra* **26**, 014015 (2019).
- <sup>67</sup>V. Gupta, H. Ganegoda, M. H. Engelhard, J. Terry, and M. R. Linford, *J. Chem. Educ.* **91**, 232 (2014).
- <sup>68</sup>N. Fairley, in *Surface Analysis by Auger and X-Ray Photoelectron Spectroscopy*, edited by D. Briggs and J. T. Grant (IMP Publications, Chichester, 2004), p. 1647.
- <sup>69</sup>S. Tardio and P. J. Cumpson, *Surf. Interface Anal.* **50**, 5 (2018).
- <sup>70</sup>J. Zhao, F. Gao, S. P. Pujari, H. Zuilhof, and A. V. Teplyakov, *Langmuir* **33**, 10792 (2017).
- <sup>71</sup>B. Singh, D. Velázquez, J. Terry, and M. R. Linford, *J. Electron Spectrosc. Relat. Phenom.* **197**, 112 (2014).
- <sup>72</sup>V. Jain, S. Bahr, P. Dietrich, M. Meyer, A. Thißen, and M. R. Linford, *Surf. Sci. Spectra* **26**, 014028 (2019).
- <sup>73</sup>S. Chatterjee, B. Singh, A. Diwan, Z. R. Lee, M. H. Engelhard, J. Terry, H. D. Tolley, N. B. Gallagher, and M. R. Linford, *Appl. Surf. Sci.* **433**, 994 (2018).
- <sup>74</sup>J. N. Hilfiker, N. Singh, T. Tiwald, D. Convey, S. M. Smith, J. H. Baker, and H. G. Tompkins, *Thin Solid Films* **516**, 7979 (2008).
- <sup>75</sup>D. Shah, S. Bahr, P. Dietrich, M. Meyer, A. Thißen, and M. R. Linford, *Surf. Sci. Spectra* **26**, 024009 (2019).
- <sup>76</sup>M. R. Anisur, P. C. Banerjee, C. D. Easton, and R. K. S. Raman, *Carbon* **127**, 131 (2018).
- <sup>77</sup>M. Sharifzadeh Mirshekarloo *et al.*, *ACS Sustain. Chem. Eng.* **8**, 1031 (2019).
- <sup>78</sup>D. J. Eyckens, C. L. Arnold, Ž. Simon, T. R. Gengenbach, J. Pinson, Y. A. Wickramasingha, and L. C. Henderson, “Covalent sizing surface modification as a route to improved interfacial adhesion in carbon fiber-epoxy composites,” *Compos. Part A Appl. S.* (submitted).